

PARAMETRIC DESIGNS AND WEIGHT OPTIMIZATION USING DIRECT
AND INDIRECT AERO-STRUCTURE LOAD TRANSFER METHODS

A Thesis

Submitted to the Faculty

of

Purdue University

by

Viraj D. Gandhi

In Partial Fulfillment of the

Requirements for the Degree

of

Master of Science in Mechanical Engineering

August 2019

Purdue University

Indianapolis, Indiana

THE PURDUE UNIVERSITY GRADUATE SCHOOL
STATEMENT OF COMMITTEE APPROVAL

Dr. Hamid Dalir, Co-chair

Department of Mechanical and Energy Engineering

Dr. John F. Dannenhoffer III, Co-chair

School of Mechanical and Aerospace Engineering

Dr. Carlos Larriba-Andaluz

Department of Mechanical and Energy Engineering

Approved by:

Dr. Jie Chen

Head of the Graduate Program

*“Building of science is depended on three pillars:
Discipline, Humbleness, and Regularity.*

If any of the pillars is not strong enough, your building will collapse on your head.”

– High school Wall

ACKNOWLEDGMENTS

I want to start with my advisors Dr. Hamid Dalir and Dr. John F. Dannenhoffer III for their continuous motivation, support, and guidance throughout my research work. I would also like to thank the member of the advisory committee, Dr. Carlos Larriba-Andaluz, for his insightful feedback and encouragement which incited me to widen my research from various perspectives.

I express special appreciation to Mr. Christian Aparicio and Mr. Julien Chaussee for their valuable inputs toward various types of analysis of different parts; Ranu Lavande for discussions related to creating API using C language and John Joe for stimulating technical conversation as well as being my all-time competitor.

Additionally, I am grateful to all my colleagues at Advanced Composite Structures Engineering Laboratory (ACSEL) for their support and keeping me sane; Udit Shah for always motivating me (directly and indirectly) throughout my undergraduate and graduate studies.

I would like to thank Mr. Jerry Mooney for his tireless efforts in reading this thesis, catching typo's and sentences which sounded like they were written at 4 A.M.

This work was funded by the CAPS project, which was funded under AFRL Contract FA8050-14-C-2472: CAPS: Computational Aircraft Prototype Syntheses; Dr. Dean Bryson is the Technical Monitor. I would like to acknowledge the discussions with Dr. Nitin Bhagat, research engineer and AFRL contractor at the University of Dayton Research Institute during the formulation of various parts of these aircraft models.

Lastly, I would like to express my gratitude towards my parents who supported me emotionally, financially and spiritually during my graduate study and in my life in general. Special thanks to my brother for standing by me and having my back during all the hardships.

TABLE OF CONTENTS

	Page
LIST OF TABLES	viii
LIST OF FIGURES	ix
SYMBOLS	xi
ABBREVIATIONS	xii
NOMENCLATURE	xiii
ABSTRACT	xiv
1 INTRODUCTION	1
1.1 Aerodynamic Load Transfer on The Structure	1
1.2 Parametric Design and Optimization	2
1.3 Motivation	3
2 REVIEW OF LITERATURE	5
2.1 Fluid Analysis	5
2.1.1 Boundary Layer Thickness	5
2.1.2 Governing Equations	6
2.1.3 Turbulence Modeling	7
2.1.4 Fluid-Structure Interaction	11
2.1.5 Prediction of Lift	14
2.2 Structural Analysis	15
2.2.1 Multipoint Constraint Element	15
2.2.2 Nastran File Structure	17
2.2.3 Nastran Cards	19
2.2.4 Optimization Solver	21
2.3 Parametric Designs	21
2.3.1 Engineering SketchPad	22

	Page
2.3.2	Naca 4-digit Airfoil Generation 22
2.3.3	Attributes in ESP 25
2.3.4	Buildup Element Model 26
3	COMPARISON OF DIRECT AND INDIRECT AERO-STRUCTURE LOAD TRANSFER METHOD 27
3.1	Fluid Analysis 27
3.1.1	Geometry of Wing 27
3.1.2	Fluid Domain and Mesh 27
3.1.3	Boundary Conditions 31
3.1.4	Convergence Check and Comparison 32
3.2	Structural Analysis 34
3.2.1	Geometry 34
3.2.2	Mesh 35
3.2.3	Material and Properties 35
3.2.4	Loads on The Wing 36
3.3	Load Transfer Using FSI 36
3.4	Load Transfer Using Stick Model 37
3.5	Result and Comparison 43
3.6	Conclusion 44
4	WEIGHT OPTIMIZATION OF WING USING INDIRECT LOAD TRANS- FER METHOD 50
4.1	User Inputs 50
4.2	Geometry Script 51
4.3	Analysis Setup 54
4.3.1	Static Structural Failure Mode 55
4.3.2	Buckling Failure Mode 57
4.4	Results 59
4.5	Conclusion 61

	Page
5 PARAMETRIC DESIGN OF AIRCRAFT USING ENGINEERING SKETCH-PAD (ESP)	64
5.1 Military Aircraft Prototype Syntheses	64
6 CONCLUSIONS AND FUTURE WORK	72
6.1 Conclusion	72
6.2 Future Scope	72
REFERENCES	74

LIST OF TABLES

Table	Page
3.1 Convergence Check (Growth Rate Change)	33
3.2 Convergence Check (Boundary Layer Height Change)	33
3.3 Comparison With XFLR5	33
3.4 Total Load Data	40
3.5 Difference in Maximum Deformation	44
4.1 Design Parameters of Wing and Panels	53
4.2 Results of Optimized Geometry	60
5.1 Design Parameters	67
5.2 Design Parameters for Figure 5.8	69

LIST OF FIGURES

Figure	Page
2.1 Boundary Layer Thickness	6
2.2 Transferring Node Data to Face Data	12
2.3 General Grid Interface Mapping	14
2.4 Load Transfer to CG	16
2.5 Force and Moment Distribution	17
2.6 Nastran File Structure	18
2.7 Airfoil Nomenclature	23
2.8 Points Distribution	26
3.1 Wing Geometry	28
3.2 Fluid Domain Surrounding Wing	29
3.3 Mesh Around the Airfoil	30
3.4 Mesh Near Surface of Wing	30
3.5 Boundary Conditions of Fluid Domain	31
3.6 Pressure Contours on The Wing and XY Plane at $Z = 5\text{m}$	32
3.7 Wing With Internal Structure	34
3.8 Structural Mesh Near Leading Edge	35
3.9 Load Transfer Using FSI	37
3.10 Pressure Center of Sections	39
3.11 Load Transfer from Pressure Center to Geometric Center	40
3.12 Shear-Moment-Torque	42
3.13 RBE3 on Edge of Rib	43
3.14 Load Applied Using Discretized Load Transfer Method	44
3.15 Structural Deformation Using Distributed Load Transfer Method ($\alpha = 7$)	45
3.16 Structural Deformation Using Discretized Load Transfer Method ($\alpha = 7$)	46

Figure	Page
3.17 Deformation vs Span at Leading Edge (Alfa = 7)	47
3.18 Deformation vs Span at Trailing Edge (Alfa = 7)	48
3.19 Deformation vs Span (Alfa = 4)	48
3.20 Deformation vs Span (Alfa = 0)	49
4.1 Loadcase CSV File	52
4.2 Rib Attributions	54
4.3 Example of Panel Attribution	55
4.4 Flowchart for Geometry Script	56
4.5 RBE3 Connection	57
4.6 Edge Attributions of Unstiffened and Stiffened Panel	58
4.7 Flowchart for Analysis Process	62
4.8 Optimized Upper Surface	63
4.9 Optimized Lower Surface	63
5.1 ESP Tree Structure to Generate a Military Fighter Aircraft	64
5.2 Middle Section of Aircraft	65
5.3 Solid OML	66
5.4 Waffle for Vertical Stabilizer	67
5.5 Waffle Without Vertical Stabilizer	69
5.6 Continuous Waffle	70
5.7 Internal Structure	70
5.8 Aircraft with Different Configurations	71

SYMBOLS

C_f	Empirical constant
τ_w	Shear stress rate
U_f	Frictional velocity
H	Boundary layer thickness
y_+	Height of first cell near wall
Γ	Effective diffusivity
k	Turbulence Kinetic Energy
w	Specific dissipation rate
C_l	Lift coefficient
m	mass
v	velocity

ABBREVIATIONS

attr	Attributes
CFD	Computational Fluid Dynamics
FSI	Fluid-Structure Interaction
VLM	Vortex Lattice Method
MPC	Multipoint Constraint
CG	Center of Gravity
CSG	Constructive Solid Geometry
BRep	Boundary Representation
MDAO	Multidisciplinary Design, Analysis and Optimization
EGADS	Engineering Geometry Aircraft Design System
ESP	Engineering Sketch Pad
BEM	Built Up Element Model
OpenCSM	Open-source Constructive Solid Modeler
DM	DesignModeler
SMT	Shear-Moment-Torque
OML	Outer Mold Layer
NSSE	Navier-Stoke System of Equations
RANS	Reynolds Average Navier-Stoke
DNS	Direct Numerical Solution
Tx	Translation in X axis
Rx	Rotation in X axis
GGI	General Grid Interface
CAPS	Computational Aircraft Prototype Syntheses
UDP	User-Defined Primitive

NOMENCLATURE

Alfa	Angle of attack
.bdf	Nastran analysis deck
Chord line	a straight line joining leading edge and trailing edge in airfoil
Camber line	halfway line between upper and lower surface
Camber (local)	Distance between camber line and chord line

ABSTRACT

Gandhi, Viraj D. M.S.M.E., Purdue University, August 2019. Parametric Designs and Weight Optimization Using Direct and Indirect Aero-Structure Load Transfer Methods. Major Professors: Dr. Hamid Dalir and Dr. John F. Dannenhoffer III.

Within the aerospace design, analysis and optimization community, there is an increasing demand to finalize the preliminary design phase of the wing as quickly as possible without losing much on accuracy. This includes rapid generation of designs, an early adaption of higher fidelity models and automation in structural analysis of the internal structure of the wing. To perform the structural analysis, the aerodynamic load can be transferred to the wing using many different methods. Generally, for preliminary analysis, indirect load transfer method is used and for detailed analysis, direct load transfer method is used. For the indirect load transfer method, load is discretized using shear-moment-torque (SMT) curve and applied to ribs of the wing. For the direct load transfer method, the load is distributed using one-way Fluid-Structure Interaction (FSI) and applied to the skin of the wing. In this research, structural analysis is performed using both methods and the nodal displacement is compared. Further, to optimize the internal structure, iterative changes are made in the number of structural members. To accommodate these changes in geometry as quickly as possible, the parametric design method is used through Engineering SketchPad (ESP). ESP can also provide attributions the geometric feature and generate multi-fidelity models consistently. ESP can generate the Nastran mesh file (.bdf) with the nodes and the elements grouped according to their geometric attributes. In this research, utilizing the attributions and consistency in multi-fidelity models an API is created between ESP and Nastran to automatize the multi-fidelity structural optimization. This API generates the design with appropriate parameters

and mesh file using ESP. Through the attribution in the mesh file, the API works as a pre-processor to apply material properties, boundary condition, and optimization parameters. The API sends the mesh file to Nastran and reads the results file to iterate the number of the structural member in design. The result file is also used to transfer the nodal deformation from lower-order fidelity structural models onto the higher-order ones to have multi-fidelity optimization. Here, static structural optimization on the whole wing serves as lower fidelity model and buckling optimization on each stiffened panel serves as higher fidelity model. To further extend this idea, a parametric model of the whole aircraft is also created.

1. INTRODUCTION

In a broad way, the objective of this research is to create a tool that can optimize the structural aspects of the preliminary design of the whole aircraft by executing a single file. Here, as the optimization needs to be done for the preliminary design phase, it should be as quickly as possible without losing much on accuracy. To achieve the goal, the project is divided into three main steps. 1) Check the reliability of discretized load transfer method; 2) Optimize the internal structure of the wing as a proof of concept; 3) Expand the 2nd step for the whole aircraft.

1.1 Aerodynamic Load Transfer on The Structure

For the purpose of structural analysis, there are many ways to transfer the aerodynamic load to structure which is mainly divided into two categories; direct and indirect load transfer. Selection of the method depends upon design phase, geometry and amount of accuracy required. Indirect method can be considered as a discretized load transfer method because the loads are applied discretely on the structural members. While the direct method can be considered as a distributed load transfer method as loads are applied on each node of the skin.

For the preliminary design phase, the indirect load transfer method is generally used. In this method, the aerodynamic geometry is divided into several sections and the loads on each section is concentrated on a single node. By connecting the nodes, a stick model representation is created. Aerodynamics team gives this data to structural analysis team and then the load is redistributed on the structural members. All these conversions might result in compromising the localized accuracy.

For distributed load transfer, Fluid Structure Interaction (FSI) technique is used. There are two main techniques of coupling fluid with the structure, fully coupled and

another is partially coupled. In the fully coupled analysis, equations of structural analysis are incorporated into the fluid analysis and behavior of the whole system is calculated simultaneously. This method is generally tailored to the problem and not typically used in industry even for the final design phase. In the partially coupled analysis, structural analysis lags behind the fluid analysis. To perform partially coupled analysis, the first step is to perform fluid analysis. Then the contact surface between the fluid domain and the structure is identified. The required data is then transferred to the structural surface from the fluid domain using different algorithms (algorithm depends on the type of data being transferred). The structural analysis is performed to calculate the deformation of nodes. In one-way FSI, the analysis ends here but in two-way FSI, the deformation from the structural analysis is transferred to the fluid domain. The mesh of fluid domain is morphed to accommodate the structural displacement and the fluid analysis is performed again. For steady state case, and the loop continues till equilibrium is achieved. For unsteady state case, it continues till given loop iterations.

In this research, the structural response of the wing is compared between stick-model method and one-way FSI method. In both methods, the underlying assumption is that the wing is a semi-rigid structure. Which means that the structure is rigid till all the load is applied and then it deforms [1].

1.2 Parametric Design and Optimization

In the design, analysis, and optimization of aerospace vehicles and structures, it is absolutely crucial to generate the geometry fast and in a robust way [2]. For a given aerodynamic geometry, the number of structural solutions to support the design are unlimited. However, there is only one solution which could lead to the minimum weight for the structure. To realize this, a single common consistent parametric description of the design against different disciplines is necessary.

In Multi-Disciplinary Analysis and Optimization (MDAO) environments, it is a common practice to import the models from manufacturing design tools with usually IGES and STEP extensions. Although these structural parts and components are intended to be ultimately manufactured, the use of these extensions will create static (non-parametric) geometry models. These models cannot be used to optimize discontinuous design variables such as the number of stiffeners. Also to create a Boundary Representation (BRep), the models should be closed watertight which is extremely difficult due to the lack of a complete solid modeling geometry kernel to deal with the topology data if any [3].

A web-browser based integrated software referred to as the Engineering Sketch Pad (ESP) [3], is used here which completely resolves the issues mentioned above. ESP is parametric design software which creates a design using CSM script file. The script file is in ASCII format and can be read using any text editors. The ESP can be coupled with many analysis software using its ability to attribute geometric feature.

In this research, the ESP is used to generate parametric designs and to generate Nastran analysis deck file. This deck file contains only mesh data and related attributions. This file is then edited and sent to Nastran to perform the required analysis. The generation of CSM script and communication between ESP and Nastran is carried out by in-house C program API. User needs to provide aerodynamic parameters and structural parameters in a comma separated variable (CSV) file. User also need to provide loadcases for which the geometry needs to be optimized in another CSV file. After providing the inputs, the user needs to execute one file to get the optimized parameters.

1.3 Motivation

The time required to finalize the internal structure of aircraft is directly impacted by the time require to make repetitive changes in design and preprocessing. The changes in designs are usually the number of structural members. Unlike thickness,

these geometric features cannot be incorporated into the stiffness matrix without physical presence. Also, if multi-disciplinary and/or multi-fidelity analysis needs to be performed, the regeneration of different models with consistent parameters is fallible and time-consuming. Thus, reduction in complexity between different models and automatization of regeneration of design is necessary. For the preprocessing, generally after iterative changes, similar mesh parameters and similar type of material properties need to be defined. There should be a way to automatize this step, too. Ultimately, an API needs to be created to connect design and analysis tools. Based on the results of the analysis, the API should be able to iterate the design also.

2. REVIEW OF LITERATURE

2.1 Fluid Analysis

In this research, Computational Fluid Dynamics (CFD) analysis is performed on the wing and the load is transferred to structural analysis. The load is transferred using two separate methods; direct load transfer method and indirect load transfer method. For the direct load transfer method, one-way Fluid-Structure Interaction (FSI) is used and for the indirect load transfer method, stick model is used. To perform analysis most accurately, the boundary layers needs to be understood properly which includes boundary layer thickness and mesh accordingly, turbulence modeling and further, load transfer algorithms.

2.1.1 Boundary Layer Thickness

Boundary layer thickness is the distance from the wall to the point where the flow velocity is 99% of free stream velocity [4]. It is represented in Figure 2.1 [5]. Boundary layer height depends upon the Reynolds number, viscosity and density [6]. The calculation from empirical equations is shown below.

Empirical constant

$$C_f = \frac{0.026}{Re^{1/7}} \quad (2.1)$$

Shear stress rate

$$\tau_w = \frac{C_f \rho U_\infty^2}{2} \quad (2.2)$$

Frictional velocity

$$U_f = \sqrt{\frac{\tau_w}{\rho}} \quad (2.3)$$

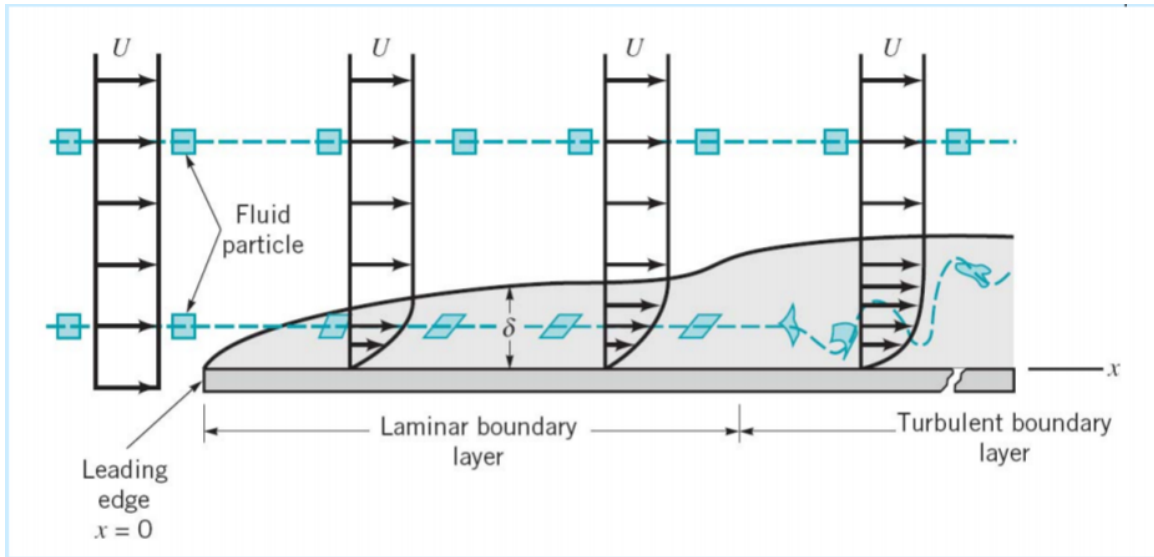


Fig. 2.1. Boundary Layer Thickness

Boundary layer height

$$\delta = \frac{\mu}{U_f \rho} \quad (2.4)$$

ρ is the density of fluid

U_∞ is the free stream velocity

μ is dynamic viscosity

In meshing terminology y_+ is the ratio of the height of first cell near the wall to boundary layer height.

2.1.2 Governing Equations

The Navier-Stokes equations govern the motion of fluids and can be seen as Newton's second law of motion for fluids. In general terms, the Navier-Stokes system of equations (NSSE) is a set of 3 equations which contains continuity equation, momentum equation, and energy conservation equation [5].

Here, the equations are given in Lagrangian (material derivative) which is represented by $\frac{D}{Dt}$ operator [5]. The conversion from Lagrangian operator to Eulerian (local derivative) is given by:

$$\frac{DQ}{Dt} = \frac{\partial Q}{\partial t} + \mathbf{u} \cdot \nabla Q \quad (2.5)$$

Continuity equation

$$\frac{D\rho}{Dt} = -\rho \nabla \cdot \mathbf{u} \quad (2.6)$$

Momentum equation

$$\rho \frac{D\mathbf{u}}{Dt} = -\nabla p + \nabla \cdot \tau'_{ij} \quad (2.7)$$

Energy equation

$$\rho \frac{De}{Dt} = \nabla \cdot (k\nabla T) - p(\nabla \cdot \mathbf{u}) + \phi \quad (2.8)$$

Here,

$$\phi = \tau'_{ij} \frac{\partial u_i}{\partial x_j} \quad (2.9)$$

$$\tau'_{ij} = 2\mu\varepsilon_{ij} + \lambda\delta_{ij}\nabla \cdot \mathbf{u} \quad (2.10)$$

Where \mathbf{u} is the fluid velocity, p is the fluid pressure, ρ is the fluid density, and μ is the fluid dynamic viscosity. τ is shear stress, κ is conductivity, e is internal energy of control volume.

These partial differential equations (PDEs) are impossible to solve analytically without certain ideal case assumptions or solve numerically. Another way to solve NSSE is by modifying them for certain flow cases which are called as turbulence modeling.

2.1.3 Turbulence Modeling

Most turbulence models are based on statistical analysis of flow which is identified as Reynolds Average Navier-Stokes (RANS) models. Selection of the model depends on the specific problem, no turbulence model is suited for every case. *k-epsilon* model predicts well far from the wall and Wilcox *k-w* model predicts well near wall. In this

research, the region near the wall as well as region far from wall needs to be solved accurately. Thus, a hybrid model which combines Wilcox $k-w$ model and $k-\epsilon$ model is used. This model is called $k-w$ SST model which has blending functions, F1 and F2 which activates necessary functions as needed [7].

Transport equation for SST $k-\omega$ model [8]

$$\frac{\partial}{\partial t}(\rho\kappa) + \frac{\partial}{\partial x_i}(\rho\kappa u_i) = \frac{\partial}{\partial x_j} \left(\Gamma_k \frac{\partial \kappa}{\partial x_j} \right) + G_\kappa - Y_\kappa + S_\kappa \quad (2.11)$$

$$\frac{\partial}{\partial t}(\rho\omega) + \frac{\partial}{\partial x_i}(\rho\omega u_i) = \frac{\partial}{\partial x_j} \left(\Gamma_\omega \frac{\partial \omega}{\partial x_j} \right) + G_\omega - Y_\omega + S_\omega \quad (2.12)$$

G_κ represents the generation of turbulence kinetic energy due to mean velocity gradients

G_ω represents the generation of specific dissipation rate

Γ_ω and Γ_κ represent the effective diffusivity of κ and ω , respectively

Y_κ and Y_ω represent the dissipation of κ and ω due to turbulence

S_κ and S_ω are user-defined source terms

D_ω represents the cross-diffusion term

Modeling the Effective Diffusivity

The terms appeared in the equation can be calculated from:

$$\Gamma_\kappa = \mu + \frac{\mu_t}{\sigma_\kappa} \quad (2.13)$$

$$\Gamma_\omega = \mu + \frac{\mu_t}{\sigma_\omega} \quad (2.14)$$

Where σ_κ and σ_ω are the turbulent Prandtl numbers for κ and ω , respectively.

μ is dynamic viscosity

The turbulent viscosity, μ_t is computed as follows

$$\mu_t = \frac{\rho\kappa}{\omega} \frac{1}{\max \left[\frac{1}{\alpha^*}, \frac{\Omega F_2}{\omega a_1} \right]} \quad (2.15)$$

Where,

$$\Omega \equiv \sqrt{2\Omega_{ij}\Omega_{ij}} \quad (2.16)$$

$$\sigma_\kappa = \frac{1}{F_1/\sigma_{\kappa,1} + (1 - F_1)/\sigma_{\kappa,2}} \quad (2.17)$$

$$\sigma_\omega = \frac{1}{F_2/\sigma_{\omega,1} + (1 - F_2)/\sigma_{\omega,2}} \quad (2.18)$$

Ω_{ij} is the mean rate-of-rotation tensor and α^* is equals to 1 for high Reynolds number

The blending functions, $F1$ and $F2$, are given by

$$F_1 = \tanh(\Phi_1^4) \quad (2.19)$$

$$\Phi_1 = \min \left[\max \left(\frac{\sqrt{\kappa}}{0.09\omega y}, \frac{500\mu}{\rho y^2 \omega} \right), \frac{4\rho\kappa}{\sigma_{\omega,2} D_\omega^+ y^2} \right] \quad (2.20)$$

$$D_\omega^+ = \max \left[2\rho \frac{1}{\sigma_{\omega,2}\omega} \frac{\partial k}{\partial x_j} \frac{\partial \omega}{\partial x_j}, 10^{-20} \right] \quad (2.21)$$

$$F_2 = \tanh(\Phi_2^4) \quad (2.22)$$

$$\Phi_2 = \max \left(\frac{2\sqrt{k}}{0.09\omega y}, \frac{500\mu}{\rho y^2 \omega} \right) \quad (2.23)$$

Where y is the distance to the next surface and D_ω^+ is the positive portion of the cross-diffusion term

Modeling the Turbulence Production

The term G_k represents the production of turbulence kinetic energy

$$G_\kappa = -\overline{\rho u_i' u_j'} \frac{\partial u_j}{\partial x_i} \quad (2.24)$$

To evaluate G_k in a manner consistent with the Boussinesq hypothesis,

$$G_\kappa = \mu_t S^2 \quad (2.25)$$

Where S is the modulus of the mean rate-of-strain tensor, defined as

$$S \equiv \sqrt{2S_{ij}S_{ij}} \quad (2.26)$$

Production of ω :

The term G_ω represents the production of ω and is given by

$$G_\omega = \frac{\alpha}{\nu_t} G_\kappa \quad (2.27)$$

Modeling the Turbulence Dissipation

Dissipation of k :

The term Y_k represents the dissipation of turbulence kinetic energy

$$Y_\kappa = \rho \beta^* \kappa \omega \quad (2.28)$$

$$\beta^* = \beta_i [1 + 1.5F(M_t)] \quad (2.29)$$

$$F(M_t) = \begin{cases} 0 & M_t \leq M_{t0} \\ M_t^2 - M_{t0}^2 & M_t > M_{t0} \end{cases} \quad (2.30)$$

Where,

$$M_t^2 \equiv \frac{2k}{a^2} \quad (2.31)$$

$$M_{t0} = 0.25 \quad (2.32)$$

$$a = \sqrt{\gamma RT} \quad (2.33)$$

$$\beta_i = F_i \beta_{i,1} + (1 - F_i) \beta_{i,2} \quad (2.34)$$

Cross-Diffusion Modification

The SST $k - \omega$ model is based on both the standard $k - \omega$ model and the standard $k - \epsilon$ model. To blend these two models together, the standard $k - \epsilon$ model has been transformed into equations based on k and ω , which leads to the introduction of a cross-diffusion term D_ω .

$$D_\omega = 2(1 - F_1)\rho\sigma_{\omega,2}\frac{1}{\omega}\frac{\partial\kappa}{\partial x_j}\frac{\partial\omega}{\partial x_j} \quad (2.35)$$

Model Constants

$$\sigma_{k,1} = 1.176, \quad \sigma_{\omega,1} = 2.0, \quad \sigma_{k,2} = 1.0, \quad \sigma_{\omega,2} = 1.168$$

$$a_1 = 0.31, \quad \beta_{i,1} = 0.075, \quad \beta_{i,2} = 0.0828$$

2.1.4 Fluid-Structure Interaction

Fluid-structure interaction is the interaction or direct data transfer between deformable structure and the fluid which share the same surface [9]. This interaction can be one way or two way. Several steps are required to transfer the data between multi-physics simulations which includes mapping of mesh, interpolation algorithms, mesh morphing, etc. Depending upon the type of properties needs to be transferred, different mapping algorithms and data transfer algorithms need to be used. In this simulation, the pressure is transferred from fluid simulation to structure simulation. For that, Conservative Profile Preserving method is used.

Conservative profile preservation

Conservative profile preserving data transfer algorithm ensures that the values of transferred properties are conserved on the target side locally (or in the vicinity). To ensure that, General Grid Interface (GGI) mapping is used which further, uses interpolation algorithms with weight functions [10]. The first step in the conservative profile preserving algorithm is to convert node data to face data.

Conversion of node data to face data

The conservative properties are on the node. This conversion is explained by example. In Figure 2.2, the data needs to be transferred to element 'a' which is formed by node 1, 2 and 3. The name of element and the area is represented by the character in the box. Here, node 1 is shared by element a, b, c, d, and e. Thus, the effect of node 1 on element 'a' is $\left(\frac{a}{a+b+c+d+e}\right) \phi_1$. By doing similarly for others, the value on face 'a' is:

$$\left(\frac{a}{a+b+c+d+e}\right) \phi_1 + \left(\frac{a}{a+e+f+g+k}\right) \phi_2 + \left(\frac{a}{a+k+h+i+j+b}\right) \phi_3 \quad (2.36)$$

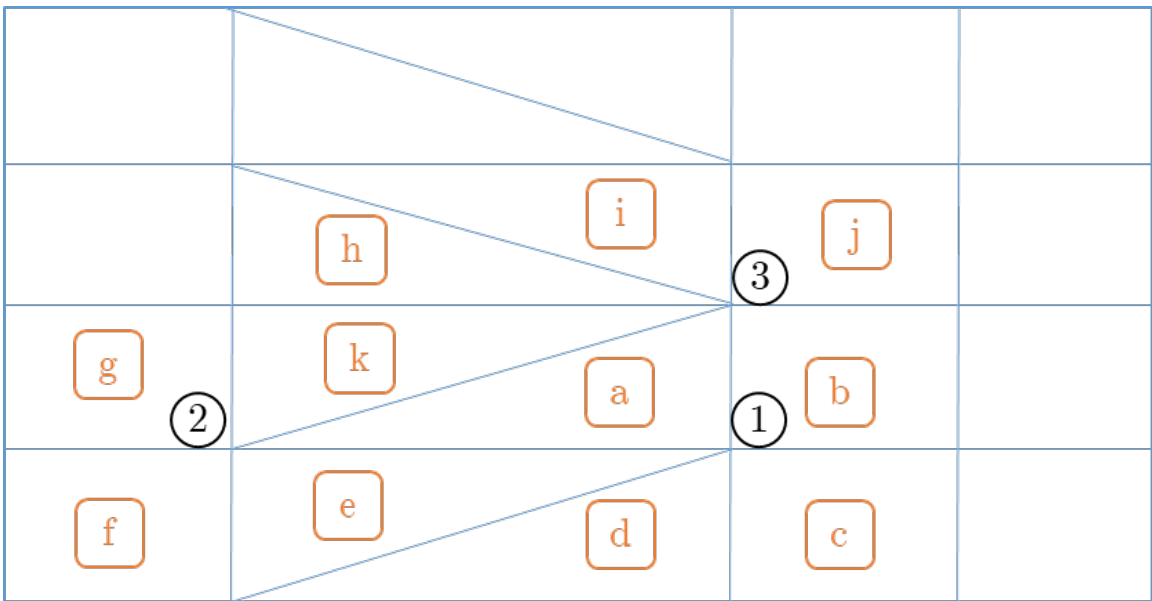


Fig. 2.2. Transferring Node Data to Face Data

General grid interface

For conservative properties, this algorithm divides faces in sub faces on both sending and receiving sides to transfer data using weighing interpolation algorithm [11].

Let's take an example shown in Figure 2.3. Here, both sides have rectangular elements which also resembles the element used in this research. The data is transferred from the CFD side to the structural side and the distance between them is zero. Initially, each element face on both sides are divided as shown. The overlapping surface of sub-faces is called 'control surface'. On the control surface, for receiving face R1, sending faces are S1 and S2. The weight of each sending face is calculated below. The convention for weight function is $W(\text{sending}, \text{receiving})$.

For face receiving face R1, sending faces are S1 and S2. From Figure 2.3, weight functions are:

$$W_{1,1} = \frac{A_1}{A_2} \quad (2.37)$$

$$W_{2,1} = \frac{A_2}{A_2 + A_3} \quad (2.38)$$

For face receiving face R2, sending faces are S2 and S3. From Figure 2.3, weight functions are:

$$W_{2,2} = \frac{A_3}{A_2 + A_3} \quad (2.39)$$

$$W_{3,2} = \frac{A_4}{A_4 + A_5} \quad (2.40)$$

Weighted interpolation algorithm

After consulting weight functions for each sending face on every receiving face, the data (ϕ) is transferred using the following equation [10]. Here, ϕ is the property being transferred and n is number of sending faces on j^{th} receiving face.

$$\phi_j = \sum_{i=1}^n W_i \phi_i \quad (2.41)$$

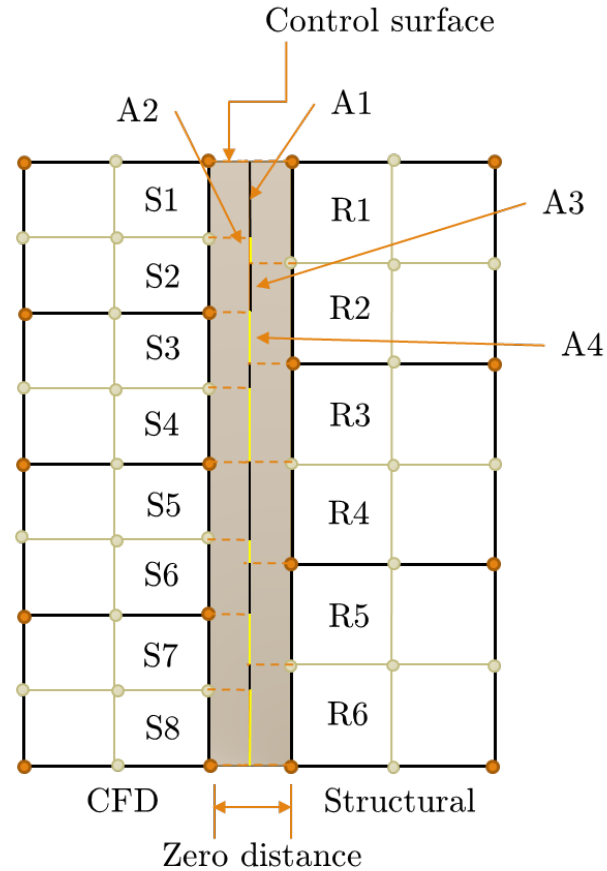


Fig. 2.3. General Grid Interface Mapping

Conversion of face data to node data

At the receiving side, the data is received as face data which needs to be converted to node data. The value of the property on each node is equal to the value of property in element divide by the number of nodes which defines the element.

2.1.5 Prediction of Lift

XFLR5 is an analysis tool which predicts the behavior of the wing using XFoils direct and inverse analysis capabilities. XFLR5 also uses the lifting line theory and Vortex Lattice Method (VLM) to get the most accurate theoretical results. The

software can generate airfoil profile and design the wing based on inverse analysis from XFOIL polar chart analysis. Although it is designed for sailplanes, the software provides ballpark values for high Reynolds number as well.

XFLR5 creates polar charts for airfoil for a range of angle of attack and range of Reynolds number. Then, the wing is created by joining two airfoils. Using polar charts and VLM, the lift coefficient at different sections of the wing is calculated. Finally, the overall lift coefficient is given as predicted coefficient of the wing [12].

2.2 Structural Analysis

In this research, structural analysis is performed on the wing using different load transfer methods. Static structural analysis is performed on the global model to get the static behavior of the wing. The edge displacement is then transferred to each panel of the wing to get local behavior. To distribute the load on ribs of the wing by indirect load transfer method, multipoint constraints (MPC) elements are used. To get the optimized thickness, Nastran DESOPT (SOL 200) is used.

2.2.1 Multipoint Constraint Element

MPC elements are used where the motion of one node is depended on the motion of at least one other node. It is also used where the load on a node is depended on at least one other node. There are many types of MPCs but here, specifically RBE3 type of MPC is used. This element does not add any stiffness to the system while RBE2 and RBAR elements add to the stiffness of the system [13].

RBE3 element

RBE3 is also identified as Interpolation Constraint Element. This element is generally used to transfer load from single point to edge or surface. For the purpose of creating an element, one master node is created at the location where the point load

data is available. This master node is connected to a group of slave nodes where the load needs to be distributed. The loads are distributed using classical bolt theory and additional weight functions of the slave nodes. After creating the element the loads are distributed using the following steps:

Step - 1: Transfer the load from the location of the master node to the center of gravity (CG) of weighted slave nodes using equivalent force/moment method. In Figure 2.4, the black dot is the location of master node, yellow is the center of gravity, blue are nodes. Bigger nodes have higher weight thus CG is transferred to the left side. Using equivalent force/moment method, the force and moment at CG is,

$$F_{cg} = F \quad (2.42)$$

$$M_{cg} = M + F.e \quad (2.43)$$



Fig. 2.4. Load Transfer to CG

Step - 2: Force on i^{th} node is applied based on the following equation. W is the weight of the node.

$$F_i = F \frac{W_i}{\sum W_j} \quad (2.44)$$

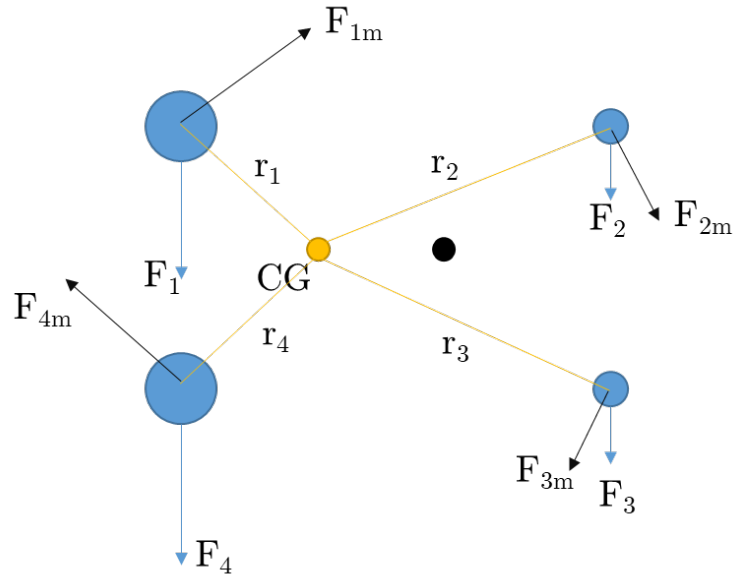


Fig. 2.5. Force and Moment Distribution

Additionally, the moment is also applied as a force perpendicular to the axis joining node and CG as shown in Figure 2.5. It is calculated from the following equation

$$F_{im} = M_{cg} \frac{W_i r_i}{\sum W_j r_j^2} \quad (2.45)$$

2.2.2 Nastran File Structure

Nastran is a structural analysis software created for NASA. It is primarily written in FORTRAN language which follows the punch card system. Which means that it has fixed size of blocks to write every command or cell size (generally 8 or 16). Here, MSC.Nastran is used for the analysis. The Nastran has three required sections which are executive control statement, case-control statements and bulk data [14]. An example is shown in Figure 2.6 where section till “CEND” is executive control statement, section till “BEGIN BULK” is case-control statement and after that, bulk data starts.

```

$ The bdf file is written by Viraj Gandhi

SOL 101
CEND

$ Direct Text Input for Global Case Control Data

ECHO = NONE
SUBCASE 1
$ Subcase name : Default
  SUBTITLE=Default
  SPC = 2
  LOAD = 2
  DISPLACEMENT(SORT1,REAL)=ALL
  SPCFORCES(SORT1,REAL)=ALL
  STRESS(SORT1,REAL,VONMISES,BILIN)=ALL

BEGIN BULK
PARAM  POST  0|
PARAM  PRTMAXIM YES
$ Elements and Element Properties for region : p1
PSHELL 1 1 .01 1 1
$ nodes
GRID 1 0 2.0116 0.0597 3.2275
GRID 2 0 2.1808 0.0572 3.8730
GRID 3 0 1.8423 0.0621 2.5820
GRID 4 0 1.6731 0.0646 1.9365
GRID 5 0 1.5038 0.0670 1.2910
GRID 6 0 1.3346 0.0694 0.6455
GRID 7 0 1.1653 0.0718 0.0000
GRID 8 0 0.7507 0.1200 0.0000

```

Fig. 2.6. Nastran File Structure

Executive control statement

In this section, the commands govern the direction of analysis. Among them, the most important is SOL command which describes which analysis to run. Here, SOL 101 is selected which is static structural analysis [15].

Case-control section

In this section, the loadcase is defined. Constrain set, load set and method of solving is described in each loadcase. Specific output file type and which property to output is also defined here. If the analysis needs to be performed for more than one loadcase, each loadcase can be performed individually using subcase command [14].

2.2.3 Nastran Cards

Nastran input files are referred to as Deck files or analysis deck. Each command in the deck is referred to as Card. The terminology comes from the punch card system where the codes were fed as a deck of cards. In this research, several cards were used which are explained below.

SOL

This is used to instruct which mode of failure needs to be analyzed. For material failure, the command is SOL 101; for stability failure, command is SOL 105. If optimization needs to be done, there needs to be two SOL cards. SOL 200 is given in executive control statement and the failure mode needs to be defined in bulk data.

SPC/Load

This is used to define the ID of the constraints and load in subcases. This ID is matched with ID in bulk data for an appropriate match.

PSHELL

This card is used to define the property of shell elements which includes property ID, material ID, and thickness.

MAT1

To define isotropic material, this card is used. Here, young modulus, shear modulus, and Poissons ratio and density of the material is defined. The ID of this card is matched with ID in PSHELL card to give appropriate property.

GRID

This card is used to generate the nodes. This card contains the node ID, the location co-ordinates and co-ordinate system to use for the location.

CQUAD4/CTRIA3

To generate element from nodes, this card is used. CQUAD4 is used to define a quad element with 4 nodes and CTRIA3 is used for triangular element with 3 nodes. The property ID is also given in this card to give the structural property of the element.

MOMENT/FORCE

This card contains node ID where force/moment is to be applied, magnitude and direction of force/moment and the load ID. This ID is to be matched with the load ID given in loadcase definition.

SPCD

This card is used to give constraints or enforced displacement to the nodes.

Optimization cards

To perform optimization, there are several other cards such as DESOBJ to define objective of optimization such as weight minimization. DVPREL1 and DESVAR is used for design variable for PSHELL thickness. DCONSTR is used to define constrain for allowable maximum stress. For buckling optimization, constrains can be given in form of the eigenvalue. Several other cards can also be used to define maximum analysis time, maximum iteration and maximum residual error.

2.2.4 Optimization Solver

Nastran optimizer is a very powerful tool which uses mathematical algorithms to minimize or maximize the required variable. Unlike other optimizers which use the design of experiment to create response surface and then perform optimization algorithms, Nastran creates response surface based on geometry, material property, loads and boundary condition [16]. Nastran uses a gradient-based optimization technique in which by default it uses conjugate gradient method. If the solver gets over-constraint, it switches to steepest descent method.

2.3 Parametric Designs

The design methodology is identified as *Parametric* when by changing one required variable, whole design can be rebuilt automatically. The variable can be number of repetition of a feature or it can be dimension. The feature can be combination of any operations. If the dimensions are interlinked, by changing one dimension others can be changed automatically. In parametric modeling, it is possible because the model saves the history of the steps so that if the change is requested, the model can repeat the process using new variables. If the model made using synchronous modeling method, it is a very tedious process for the designer to change one parameter [17]. There are two popular parametric representation models:

Constructive Solid Geometry (CSG): In this method, the model is defined using primitive and grown (extrude and sweep operation) solid shapes. The model is usually interpreted as the combination of primitive shapes and Boolean operations to get final shape.

Boundary Representation (BRep): In this method, solid is represented by surface manifold. The solid is then formed by joining the edges and nodes (here, the node is the endpoint of edges). As the operations are carried by surface tessellation, volume mesh can be easily controlled [18].

2.3.1 Engineering SketchPad

Engineering SketchPad (ESP) is a solid-modeling, feature-based, web-enabled system for building parametric geometry [3]. ESP is built upon the WebViewer [3] and OpenCSM [19] and is fully-parametric, attributed and is based on a feature-based solid-modeling system. OpenCSM, in turn, is built upon Engineering Geometry Aerospace Design System (EGADS) [20] and OpenCASCADE. The underlying objective of ESP is to be able to create geometry for multidisciplinary design, analysis and optimization (MDAO) which leads to creating multi-fidelity geometry which shares the same dimension.

ESP uses CSG manipulation to generate geometry because it uses design-gradient information for optimization. It uses openCASCADE open-source solid-modeling geometry kernel to support CSG [21].

For MDAO and CSG, usually bottom-up and potentially mixed with the top-down approach is used. To do that, a new software suite, EGADS is developed [20]. It is an object-based API to communicate between geometry kernel openCASCADE and GUI of ESP where the functionality is focused on building multi-fidelity, parametric, geometric models for design.

2.3.2 Naca 4-digit Airfoil Generation

One of the best example to understand the importance of EGADS is through airfoil creation. For the user, an airfoil is created using the command line: “udprim naca Series 4412 sharpte 1”. Here, the line is calling NACA user defined primitive (UDP), to generate NACA 4412 series airfoil with sharp tail enabled. Using this information, EGADS submits a group of points to openCASCADE to join them using a 2^{nd} degree polynomial curve. One curve is created for upper edge and another curve for lower edge. Both curves are then concatenated to form a closed loop which is further converted to a sheet. The following section shows the calculation done by EGADS.

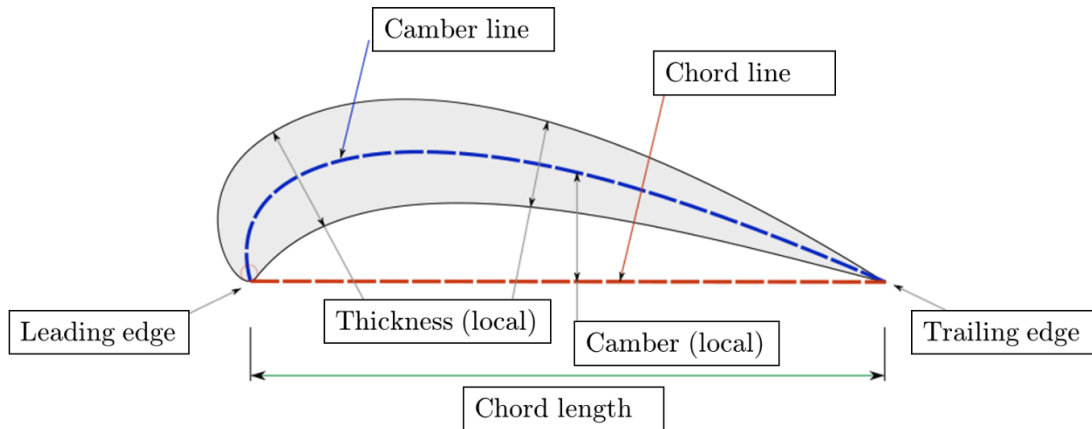


Fig. 2.7. Airfoil Nomenclature

The nomenclature is shown in Figure 2.7 [22]. The interpretation of the NACA profile is NACA MPXX where M is the maximum camber divided by 100. Here, for NACA 4412, $M=4$. So the maximum camber is 0.04 or 4% of the chord length. P divided by 10 is the position of the maximum camber. Here, $P=4$ so the maximum camber is at 0.4 or 40% of the chord length. XX divided by 100 is the thickness (T). Here, $XX=12$ so the thickness is 0.12 or 12% of the chord length. ESP creates airfoil of chord length = 1. Then it can be scaled using transformation operation.

To create the NACA profile, initially a camber line is created. Further, the thickness is distributed around the camber line. To create the final airfoil, the gradient of the camber line is also required. There are two equations for the camber line. One is for before the location of maximum camber (P) and another for the rest of the camber line. The airfoils are created in X-Y plane where X co-ordinate is in the chordwise direction. Here, Y_c and Y_t are Y co-ordinate of camber line and thickness distribution at given X. The location of points is calculated using the following equation [23].

For section $0 \leq x < P$

Camber:

$$y_c = \frac{M}{P^2}(2Px - x^2) \quad (2.46)$$

Gradient:

$$\frac{dy_c}{dx} = \frac{2M}{P^2}(P - x) \quad (2.47)$$

For section $P \leq x \leq 1$

Camber:

$$y_c = \frac{M}{(1 - P^2)}(1 - 2P + 2Px - x^2) \quad (2.48)$$

Gradient:

$$\frac{dy_c}{dx} = \frac{2M}{(1 - P^2)}(P - x) \quad (2.49)$$

Thickness:

$$y_t = \frac{T}{0.2} (a_0x^{0.5} + a_1x + a_2x^2 + a_3x^3 + a_4x^4) \quad (2.50)$$

$$a_0 = 0.2969$$

$$a_1 = -0.126$$

$$a_2 = -0.3516$$

$$a_3 = 0.2843$$

$$a_4 = -0.1036 \text{ (closed trailing edge)}$$

The position of the upper and lower surface can be calculated perpendicular to the camber line.

$$\theta = \text{atan} \frac{dy_c}{dx} \quad (2.51)$$

Upper surface:

$$x_u = x_c - y_t \sin(\theta) \quad (2.52)$$

$$y_u = y_c + y_t \cos(\theta) \quad (2.53)$$

Lower surface:

$$x_l = x_c + y_t \sin(\theta) \quad (2.54)$$

$$y_l = y_c - y_t \cos(\theta) \quad (2.55)$$

There are several ways to distribute points between 0 and 1. If the points are spread equally, there will be the same number of points at the location of high curvature (leading edge) and at the relatively flat portion. To avoid that, points are grouped on the leading edge and trailing edge using cosine distribution using the equation below [24].

$$x = 0.5(1 - \cos(\beta)) \quad (2.56)$$

$$\beta = (\text{point ID} - 1) * \frac{p}{180} \quad (2.57)$$

The distribution of points is shown in Figure 2.8. For the cosine distribution, there are 7 points between 0 and 0.1 camber line location (which is high curvature) while on equal distribution, there are only 4 points. Here, 31 points are shown for example but EGADS sends 101 points to openCASCADE to generate each edge of an airfoil.

2.3.3 Attributes in ESP

In simpler words, attributes are name/value pair that can be given to any EGADS object. Any number of attributes can be given to object. The primary use of attributes is the ability to automate the process of providing analysis parameters such as boundary conditions, material property, etc. Also, attribute makes the multi-fidelity transfer of loads and displacement between structures or models a nearly-trivial process. This feature is useful in the multi-disciplinary coupling analysis as well [2].

Attributes on geometries are consistent upon further operations [3]. For example, if a sheet with attribute Sheet-1 is intersected with a box, the intersected sheet will retain its attribute as Sheet-1. Thus, it is always preferred to provide attributes as

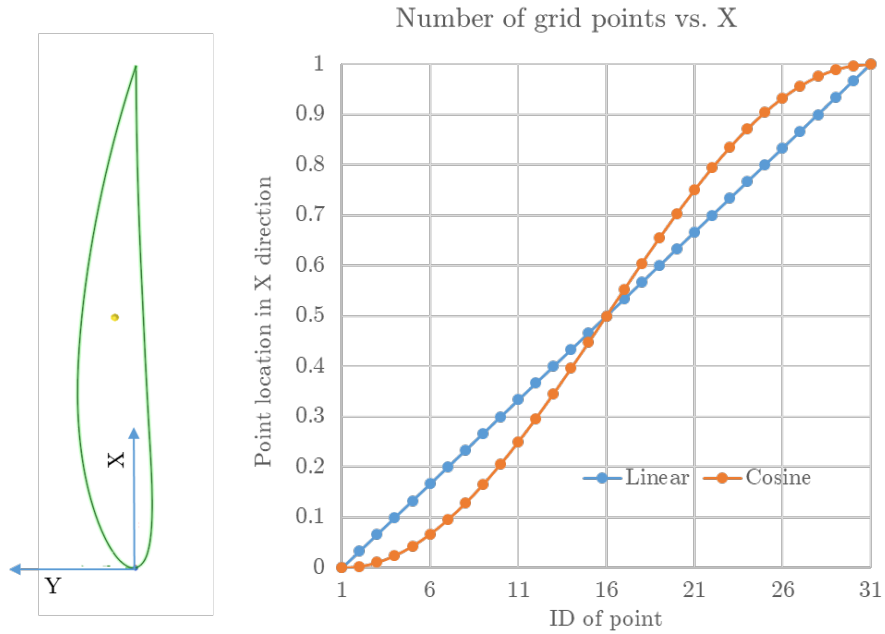


Fig. 2.8. Points Distribution

it is generated rather than selecting the geometry feature later. Attributes in the analysis system can be used by two different methods. One is direct communication with EGADS in the system memory or by dumping mesh file generated by ESP itself.

2.3.4 Buildup Element Model

ESP generates Nastran analysis deck (.bdf file) using UDP createBEM. In analysis deck, ESP groups elements and grids for each edge, surface, and volume separately. The attributes which were applied during creating the geometry are also included as comments for each group. This bdf file can be processed by an API to apply material properties and boundary conditions to elements and nodes using attributes [2].

3. COMPARISON OF DIRECT AND INDIRECT AERO-STRUCTURE LOAD TRANSFER METHOD

This chapter shows the method to convert aerodynamic load acting on the wing to discretized stick model load and how to apply it to do analysis. A complete procedure to perform CFD analysis on the wing is also illustrated. Further, the comparison of structural behavior for direct load transfer and indirect load transfer is done for the preliminary design of the wing.

3.1 Fluid Analysis

3.1.1 Geometry of Wing

To create an accurate profile of an airfoil, Engineering Sketchpad (ESP) is used. In ESP, to create the outer mold layer (OML) of the wing, two NACA 4412 airfoil profile is created at the required location and ruled. Further, the STEP file was dumped to be imported in Ansys DesignModeler (DM). The aerodynamic parameters used to create wing are: the area is 48.5 m^2 , the aspect ratio is 9.09, the taper ratio is 0.3 and the sweep angle is 30. The top view of the 3D wing is shown in Figure 3.1 and dihedral angle is zero. Here, the wing is similar to challenger 350. This is the required geometry to perform CFD analysis. The fluid domain surrounding the wing is created in DM.

3.1.2 Fluid Domain and Mesh

The size of fluid domain should be large enough that the effect of boundary on the flow can be neglected. Due to limitations in computational capabilities, some sides are given special type of boundary conditions. The dimension of fluid domain is

represented in Chord length (C) and semi-span (S) in Figure 3.2. (The image is not to scale. It is for easy representation). In the Figure 3.2, the dimensions of the sides are:

- $a = 15C$: Domain before leading edge at the root
- $b = 20C$: Domain after trailing edge at the root
- $f = 5S$: Domain is span direction
- $d = 20C$: Domain above wing
- $c = 15C$: Domain below wing

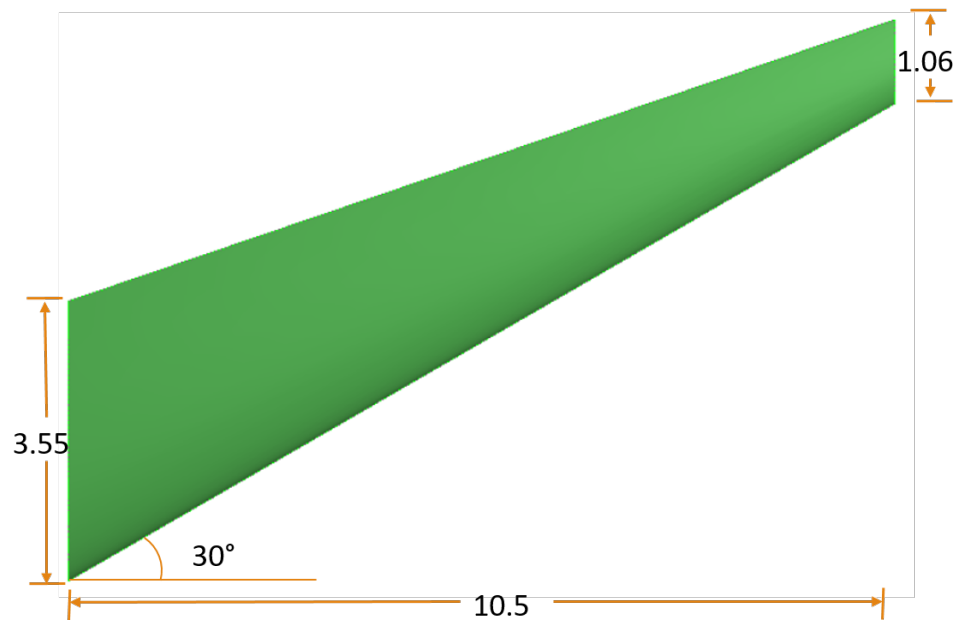


Fig. 3.1. Wing Geometry

The wing is divided into a certain number of sections in span direction. It is required for converting CFD load to stick model load in post-processing which is described in section 3.4. Value of 'd' is greater than 'e' because the wing is being simulated with angle of attack flow input. As some of the flow is going from lower domain section to upper section, it is better to have asymmetrical domain size [25].

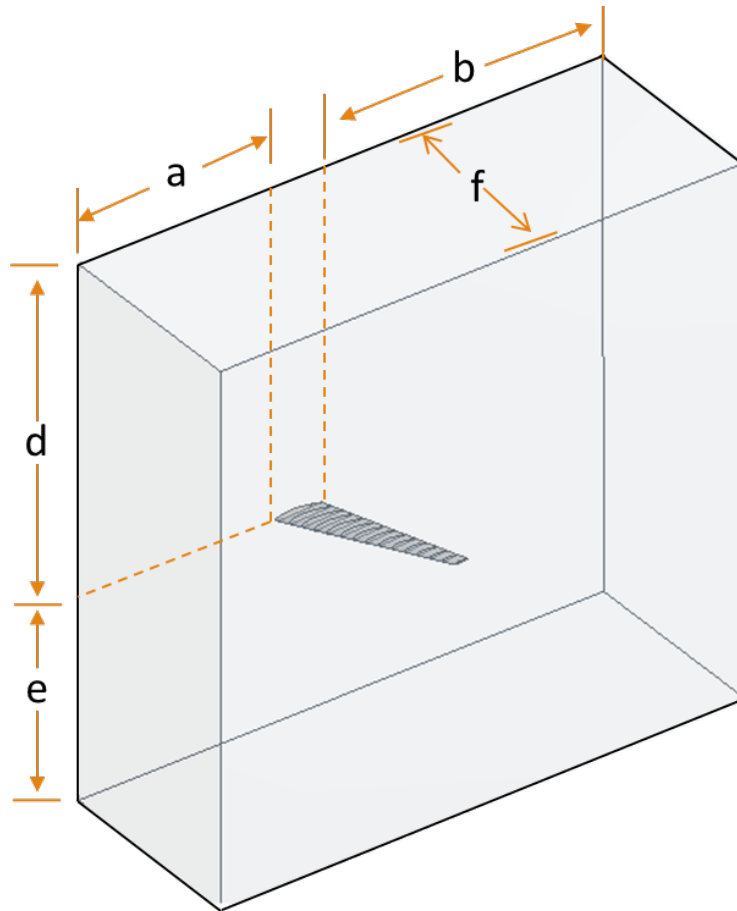


Fig. 3.2. Fluid Domain Surrounding Wing

The mesh (Figure 3.3 and Figure 3.4) is generated using boundary layer theories. As this research is mainly focused on surface pressure and shear forces, it is absolutely crucial to capture boundary layer. To do that, a certain turbulence model needs to be used which are fairly stable for maximum y^+ value between 1 and 12 [26]. Hexahedron mesh is created using Ansys ICEM module using blocks method. The Reynolds number is approximately 30×10^6 . The boundary layer thickness is 3.5×10^{-6} m. The first cell height is 15×10^{-6} m thus the y^+ value is 4.3 [6]. The growth rate is kept at 1.15 and the total elements are 20×10^6 .

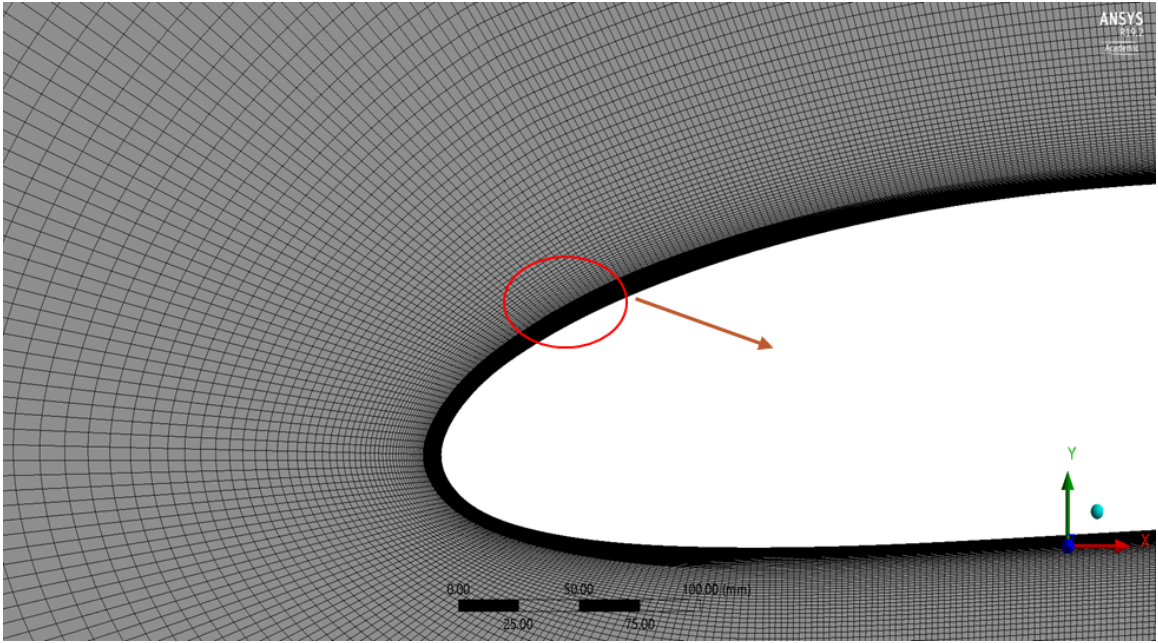


Fig. 3.3. Mesh Around the Airfoil

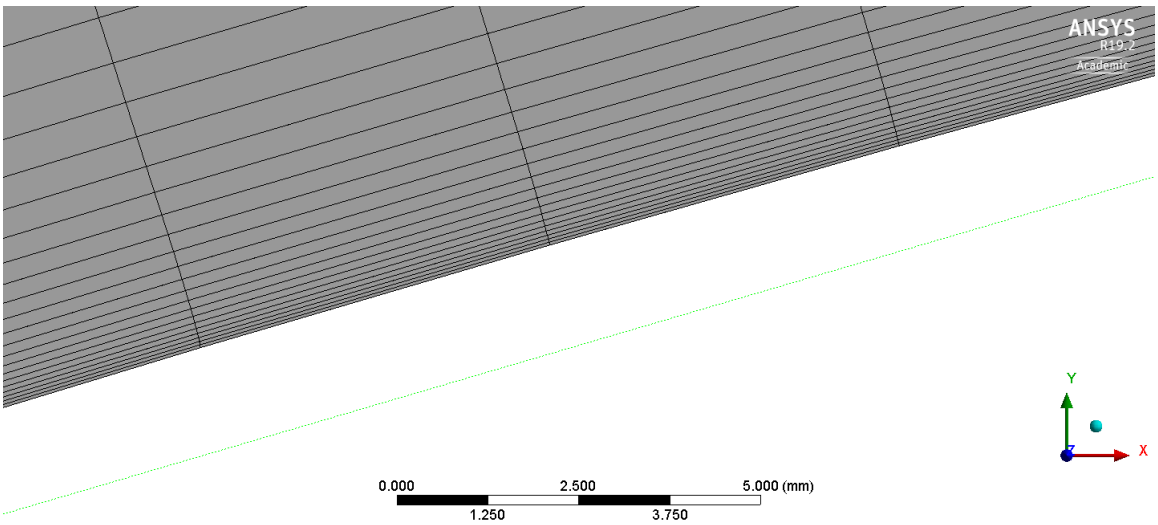


Fig. 3.4. Mesh Near Surface of Wing

3.1.3 Boundary Conditions

To simulate the flow with an angle of attack, the components of velocity is given in X and Y direction at “inlet”. The root side of the fluid domain is given symmetric condition. The back side of the domain is given outlet condition. The upper, lower and tip side of fluid domain are given open condition as shown in Figure 3.5.

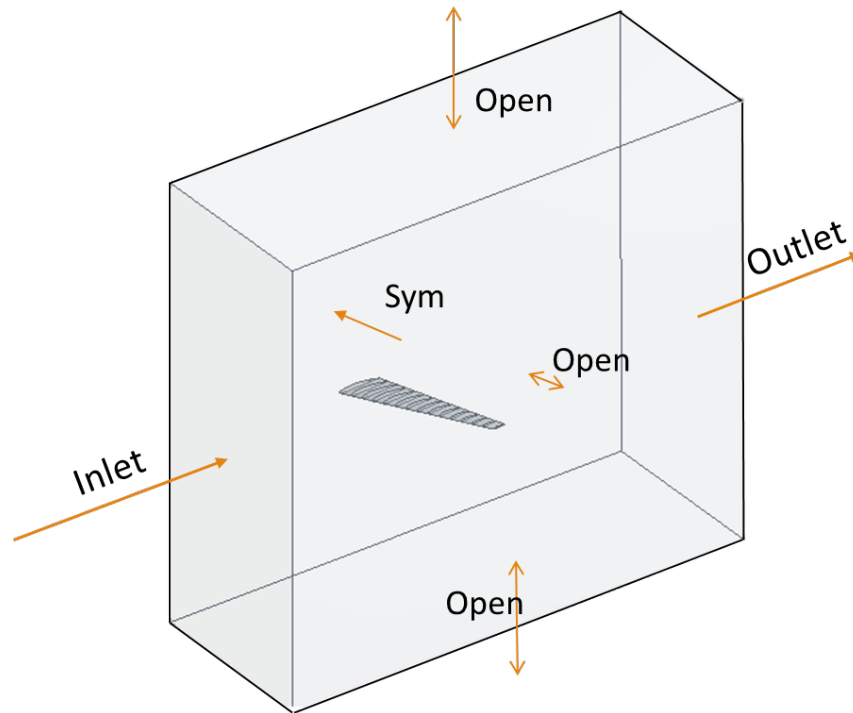


Fig. 3.5. Boundary Conditions of Fluid Domain

The open condition is given to simulate semi-infinite side. At the tip, due to vortex, the flow might enter the domain and this BC allows fluid to come in. While the pressure outlet condition works as one way valve for each individual element face [27]. This can be avoided by having a big domain but due to limitations in computational capabilities, it was not possible. The relative pressure is kept zero at the outlet and open BC side. The inlet condition is 0.35 Mach number at 7-degree angle of attack. The surface of the airfoil is a smooth wall with no-slip boundary condition.

3.1.4 Convergence Check and Comparison

As the mesh was generated using boundary layer theories, the convergence of mesh parameters was obtained fairly quickly. The initial value of first cell height 20×10^{-6} m is chosen. As the area of interest is shear forces at the surface of the wing, dominating parameters are the height of first cell near the surface and the growth rate. Table 3.1 and Table 3.2 shows convergence history and Table 3.3 shows calculated value with XFLR5. XFLR5 predicts the lift and drag coefficient of the wing. The tool can give only approximate data.

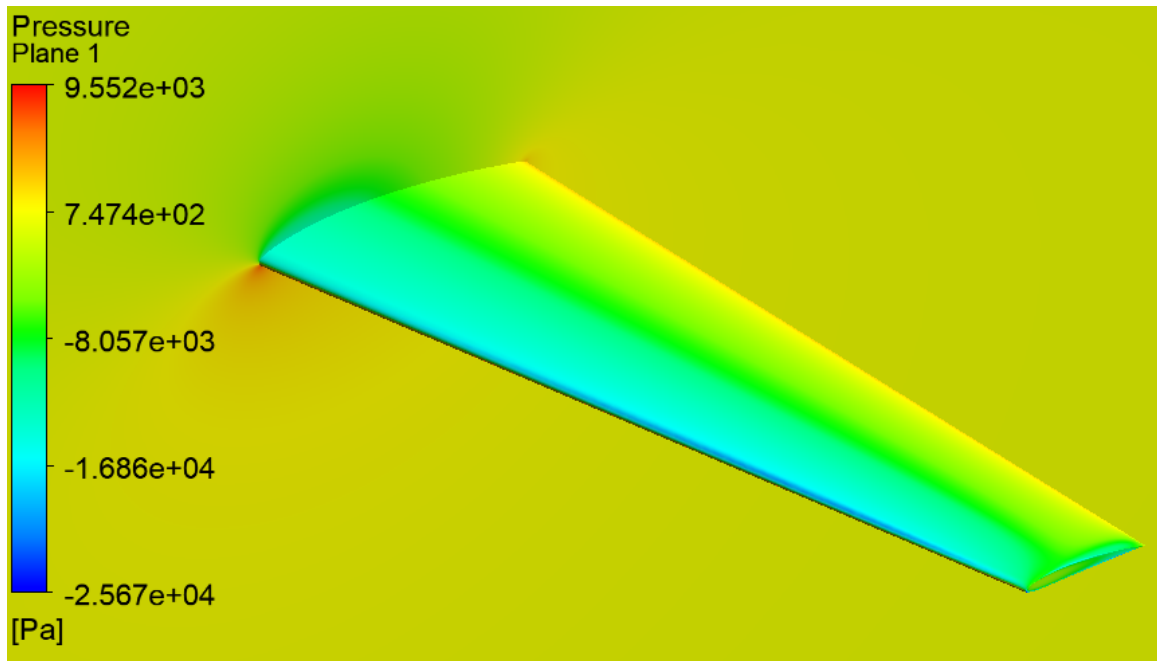


Fig. 3.6. Pressure Contours on The Wing and XY Plane at $Z = 5$ m

Table 3.1.
Convergence Check (Growth Rate Change)

Boundary layer cell height = $20 \times 10^{-6}\text{m}$	
Growth rate	C_l
1.250	0.9364
1.200	0.9312
1.150	0.9291
1.100	0.9290

Table 3.2.
Convergence Check (Boundary Layer Height Change)

For growth rate = 1.150	
Boundary layer cell height ($\times 10^{-6}\text{m}$)	C_l
20.0	0.9291
15.0	0.9283
10.0	0.9281
8.0	0.9280

Table 3.3.
Comparison With XFLR5

Alfa	CFD C_l	XFLR5 C_l
0	0.3621	0.3744
4	0.6954	0.7152
7	0.9283	0.9426

3.2 Structural Analysis

3.2.1 Geometry

The same OML is imported in another DM and the internal structures are created. The internal structure (i.e. ribs and spars) are generated by intersecting planer sheets with the solid wing OML so that the sheets get the exact profile of the wing. Then, the solid OML is converted to sheet OML. All the bodies are condensed to one part to have shared nodes between different intersecting surfaces. This will ensure the proper load transfer from the skin of the wing to the structure of the wing. Ribs are equally spaced while spars are created at 17%, 45% and 73% of chord length shown in Figure 3.7.

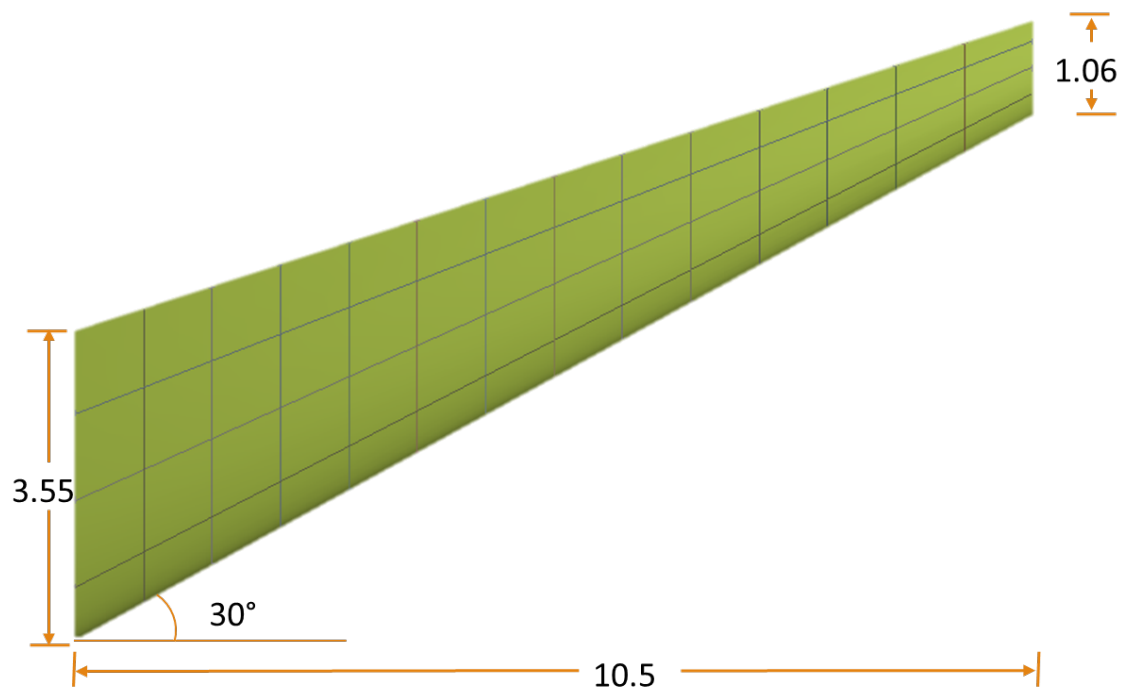


Fig. 3.7. Wing With Internal Structure

3.2.2 Mesh

For the purpose of accurate load transfer from fluid analysis to structure analysis, relatively finer mesh is used as shown in Figure 3.8. This will ensure better localized accuracy and mapping for conservative load transfer method [10]. The same mesh is used when the load is transferred by the discretized method for consistency. Mesh is considerably finer on the leading edge because of the huge change in pressure.

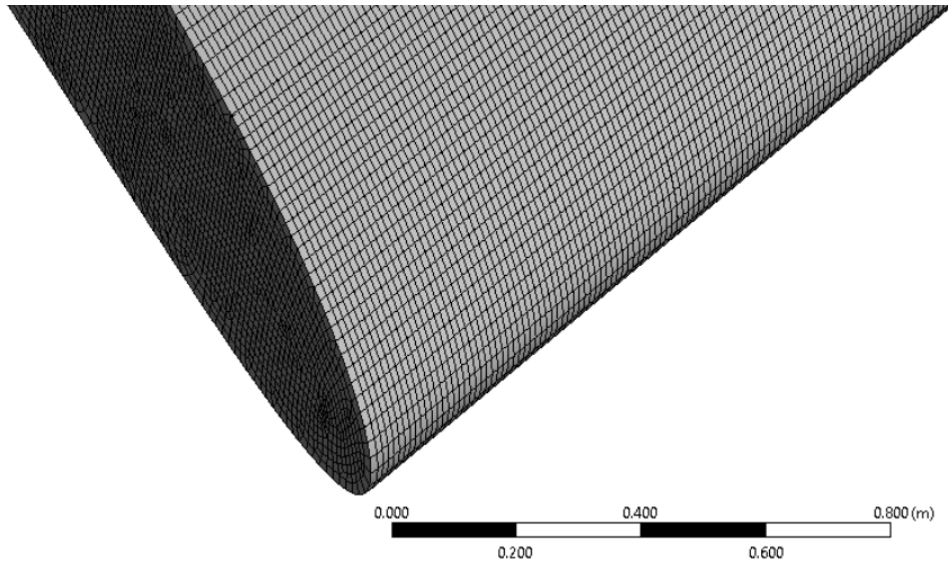


Fig. 3.8. Structural Mesh Near Leading Edge

3.2.3 Material and Properties

For all the loadcases and both load transfer methods, the same thickness and the same material is chosen. The material is Aluminium alloy which has Young modulus of 71GPa and Poisson's ratio is 0.33. The thickness is 5mm uniform.

3.2.4 Loads on The Wing

Distributed load transfer

For the distributed load transfer method, the pressure from CFD results is directly transferred to structural grid nodes. For the purpose to transfer pressure and essentially force, conservative data transfer algorithms need to be used. Here, the load will be applied to each individual nodes on the skin of the wing. The method is described in section 3.3.

Discretized load transfer

In this method, the aerodynamic load is converted into stick model load and then it is redistributed only on the edge of ribs using RBE3 elements. The master node is generally created at the geometric center which may or may not be the same as pressure or force center. The weight function for each slave node is 1. The force and moments on master nodes are calculated in section 3.4.

Boundary Condition

The root of the wing is constrained in T_x , T_y , and T_z direction. It is complex to give accurate boundary condition to a wing because, in reality, the root of the wing is transferring the load to the fuselage and eventually give translation in lift direction.

3.3 Load Transfer Using FSI

After getting the convergence of mesh and a relatively valid agreement with XFLR5 data, the load can be transferred to structural mesh. In order to do that, Ansys provides a user interface where the user needs to connect the static structural model to CFD results. The mesh mapping will be done based on overlapping surfaces within a marginal distance. The pressure data is then transferred to the required

structural nodes from the fluid nodes. There are many algorithms for data transfer and mapping. Here, as the force needs to be transferred, Conservative Profile Preserving data transfer algorithm needs to be used. The transferred load on the upper surface is shown below in Figure 3.9.

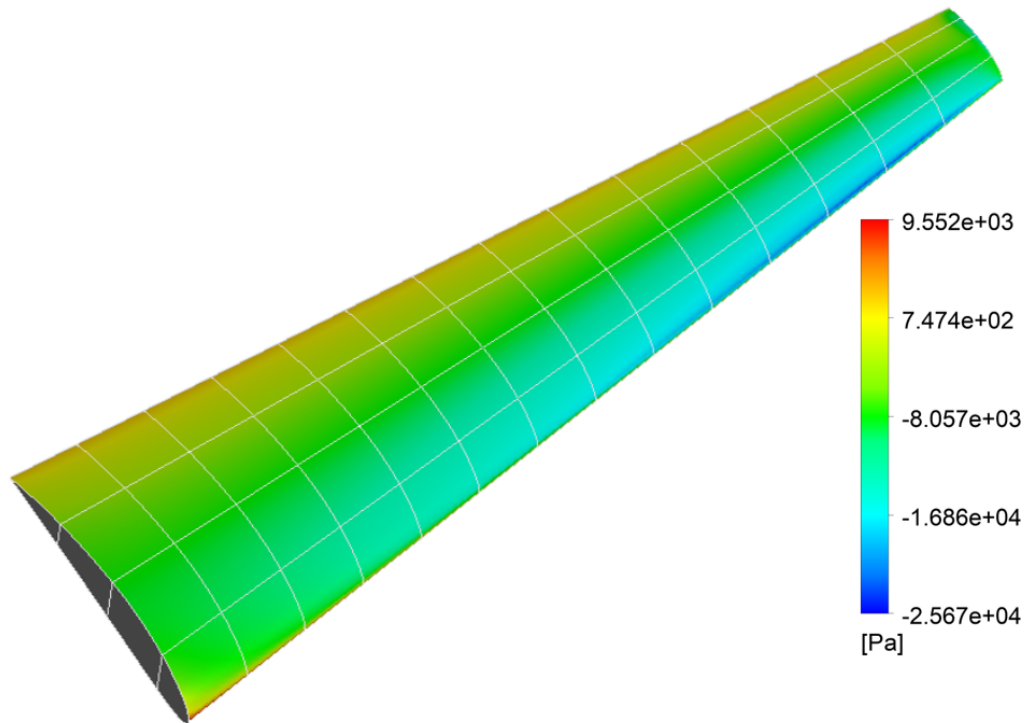


Fig. 3.9. Load Transfer Using FSI

3.4 Load Transfer Using Stick Model

To transfer the load using stick model approach, the intersection of the wing OML and fluid domain is divided into subsections as shown in Figure 3.2. The loads on these sections are calculated independently and concentrated on the geometric center of each section. This is the location of the node of stick model. A smooth curve of shear force - bending moment - torque (SMT) joining each node is created. As the

number of sections and location of stick model node is independent to the location of rib, interpolation is done to get the load data at the location of rib. This load is applied to the master node of RBE3. The whole process is shown below. The coordinate system is: +X is chordwise direction, +Z is spanwise direction and +Y is lift direction.

Step - 1: Calculate the lift acting on each section by calculating the force on each element of that section.

$$Lift = \oint P(x, z) \, dx dz \quad (3.1)$$

Step - 2: Calculate the center of pressure for each section which is denoted by Px and Pz in X and Z direction.

$$Pressure \, center \, [Px, \, Pz] = \left[\frac{\int x \, P(x, z) \, dx dz}{\int P(x, z) \, dx dz}, \frac{\int z \, P(x, z) \, dz dx}{\int P(x, z) \, dz dx} \right] \quad (3.2)$$

The representation of the center of pressure is shown in Figure 3.10. The points are not necessarily on a line.

Step - 3: In this step, the load is transferred from the pressure center to the geometric center represented in Figure 3.11. This will create moment in the Z direction and X direction. Also, the bending moment generated due to shear force in each section is calculated. The geometric center is denoted by Gx and Gz in X and Z direction. The load calculated in this step is the amount of load which is generated by the section.

Generated loads at the discretized node are:

Force in Y direction (shear force):

$$F_y = Lift - (fuel + structure \, weight) * G \quad (3.3)$$

Moment generated in Z direction (torsion):

$$M_z = - F_y * (G_x - P_x) \quad (3.4)$$

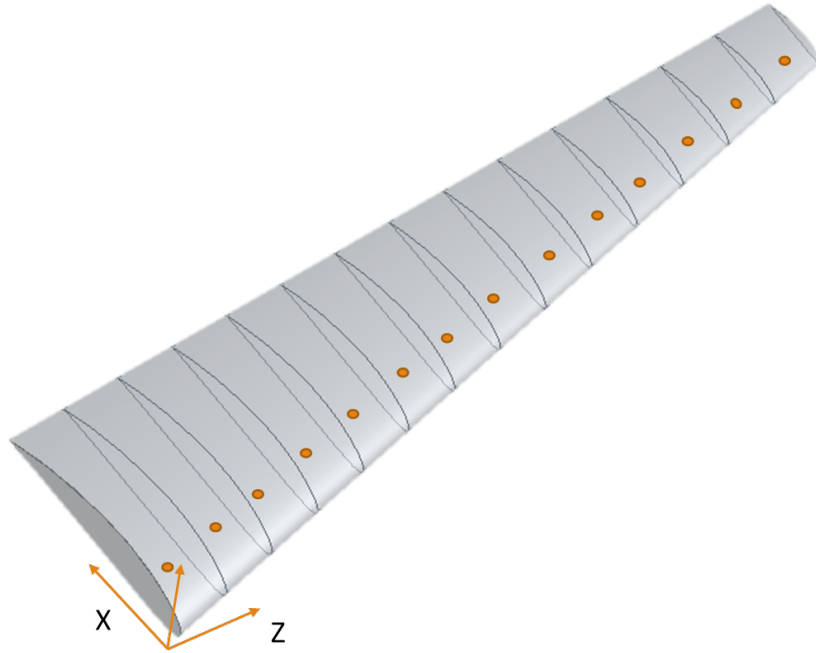


Fig. 3.10. Pressure Center of Sections

Bending moment generated in X direction due to shear force (BMSF):

$$M_x = (-F_y) * Gz \quad (3.5)$$

The moment in X due to the distance between Gz and Pz is usually very small compared to the moment generated by shear force. Thus, it is usually ignored.

G = gravity force multiplier

In moments, the negative sign comes from the direction of forces.

Step - 4: Find the total load on the wing and generate total load Vs span graph. This graph shown in Figure 3.12 is also called as SMT graph and the data is given in Table 3.4. Numbering convention on rib starts from the tip. So, the section at the tip is 1st section. The amount of total load on nth discretized node = load generated on nth discretized node + total load on (n-1)th discretized node. The example shown here is for 7 degree angle of attack at Mach number = 0.35. This represents 2.5G loadcase for bombardier challenger 350 which weighs 18,416 KG [28].

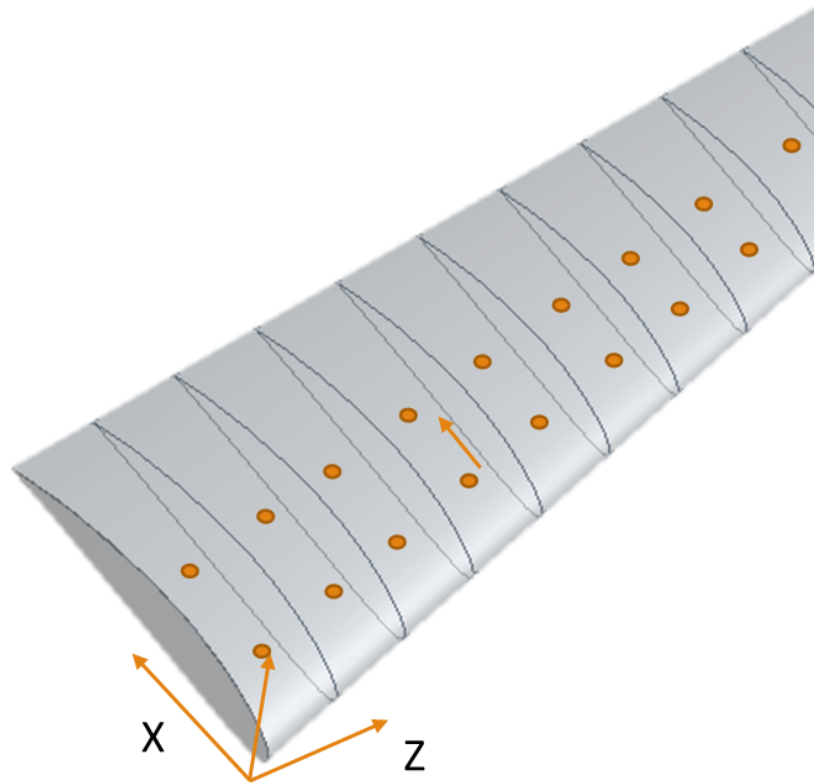


Fig. 3.11. Load Transfer from Pressure Center to Geometric Center

Here, the total M_x is around -1275 KN.m that is generated by shear force. Total moment generated by transferring F_y from P_z to G_z is 4.5 KN.m. So, it can be ignored.

Table 3.4.: Total Load Data

Span (m)	Total F_y (N)	Total M_z (N.m)	Total M_x (N.m)
0.375913	215450.4	-70319.3	-1276262.47
1.12542	208377.5	-69087.3	-1273603.66
1.874597	198589.8	-66794	-1262588.4

continued on next page

Table 3.4.: *continued*

Span (m)	Total Fy (N)	Total Mz (N.m)	Total Mx (N.m)
2.623899	187044	-63804.7	-1240944.69
3.373339	174103.6	-60129.7	-1206990.41
4.122748	159953.8	-55767.4	-1159258.37
4.872148	144726.7	-50723.2	-1096480.89
5.62156	128541.1	-45016.6	-1017622.42
6.370835	111518.2	-38686.7	-921926.834
7.119978	93783.02	-31797.6	-808939.167
7.868783	75472.9	-24449.6	-678571.469
8.616797	56742.79	-16797.3	-531188.324
9.361831	37774.46	-9102.14	-367742.07
10.11266	18784.47	-1869.56	-189960.999

Step - 5: The aerodynamics department gives the graph generated above to the structural analysis department. To perform structural analysis, interpolation needs to be done at the rib location to get the total load. Here, the numbering starts from the tip. The tip rib being external is given number '0'. One thing to notice in the graph is it doesn't end at tip location nor it starts from the root. The amount of total load on 0th rib is given below.

$$\text{Total load on } 0^{\text{th}} \text{ rib} = \text{load on } 1^{\text{st}} \text{ discretized node} * \frac{a}{\text{width of section}} \quad (3.6)$$

$a = \min$ (distance between 1st rib to 1st discretized node, width of section)

If the width of the section is not known by the structural analysis team, the load on 0th rib is half of the load on 1st discretized node.

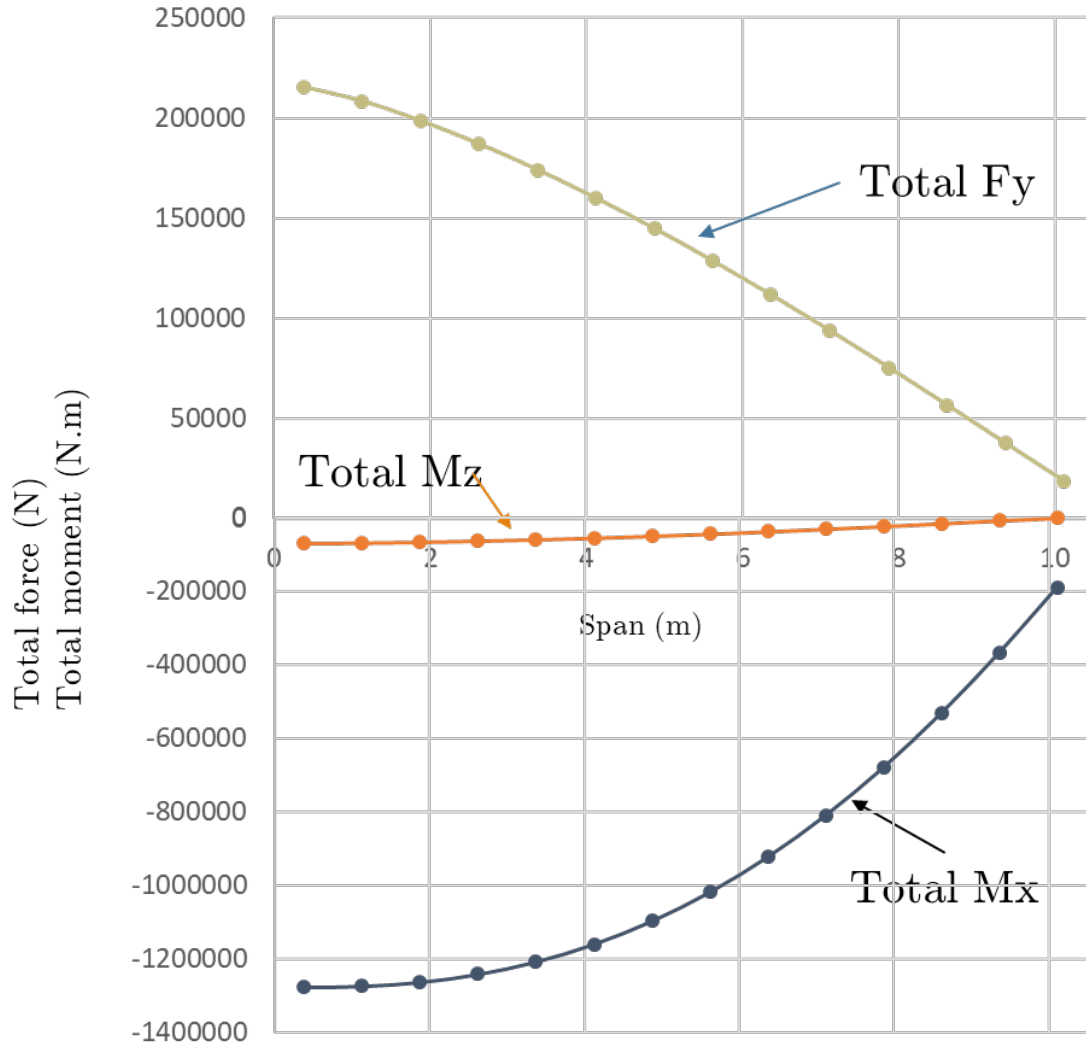


Fig. 3.12. Shear-Moment-Torque

Step - 6: Now, the total load needs to be converted to the applicable load on each rib. For the 0th rib, the applicable load is equal to the total load. For nth rib, the equations are listed below.

For shear force (Fy):

$$\text{applicable } Fy \text{ on } n^{\text{th}} \text{ rib} = \text{total } Fy \text{ on } n^{\text{th}} \text{ rib} - \text{total } Fy \text{ on } (n - 1)^{\text{th}} \text{ rib} \quad (3.7)$$

For torsion (Mz):

$$\text{applicable } Mz \text{ on } n^{\text{th}} \text{ rib} = \text{total } Mz \text{ on } n^{\text{th}} \text{ rib} - \text{total } Mz \text{ on } (n - 1)^{\text{th}} \text{ rib} \quad (3.8)$$

For bending moment (Mx):

$$\text{applied } Mx \text{ on } n^{\text{th}} \text{ rib} = \text{total } Mx \text{ on } n^{\text{th}} \text{ rib} - BMSF \quad (3.9)$$

These loads are applied to master node on RBE3 elements of ribs. The RBE3 elements are represented in Figure 3.13. The discretized load on wing is represented in Figure 3.14. Here, the skin is hidden.

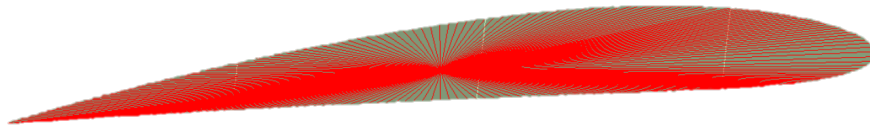


Fig. 3.13. RBE3 on Edge of Rib

3.5 Result and Comparison

For comparison, 3 loadcases are analyzed. One is critical loadcase that is at 7 degree angle of attack which replicates 2.5 G at taking off; another is 4 degree angle of attack which replicates 1.6 G; the last is 0 degree angle of attack which replicates 1 G cruising. In all the cases, the Mach number is kept fixed at 0.35. The deformation from the leading edge and the trailing edge is taken as output and compared. Figure 3.15 and Figure 3.16 shows the deformation is similar and the graph in Figure 3.17 and Figure 3.18 agrees with that.

As it can be seen from Figure 3.17 and Figure 3.18 that both lines coincide on each other throughout the span. The difference at maximum deformation is 0.27%. Similar behavior can be seen for the other two cases as well shown in Figure 3.19 and Figure 3.20.

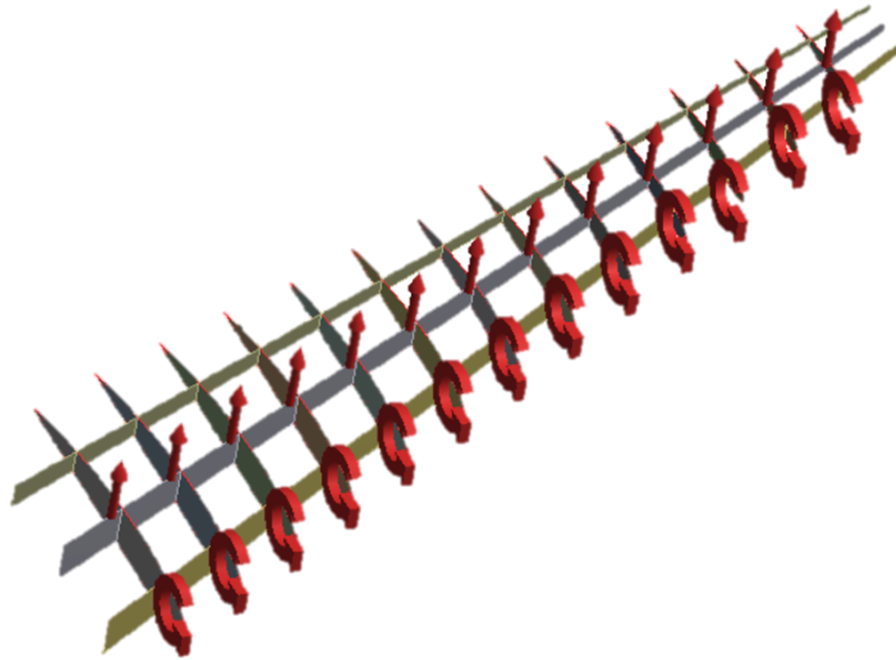


Fig. 3.14. Load Applied Using Discretized Load Transfer Method

Table 3.5.
Difference in Maximum Deformation

Alfa	Max difference (mm)	% difference at max deformation
0°	5.59	1.46
4°	2.41	0.34
7°	2.49	0.27

3.6 Conclusion

Discretized load transfer method provides results as accurately as distributed load transfer method up to at least 9.09 aspect ratio for preliminary design phase.

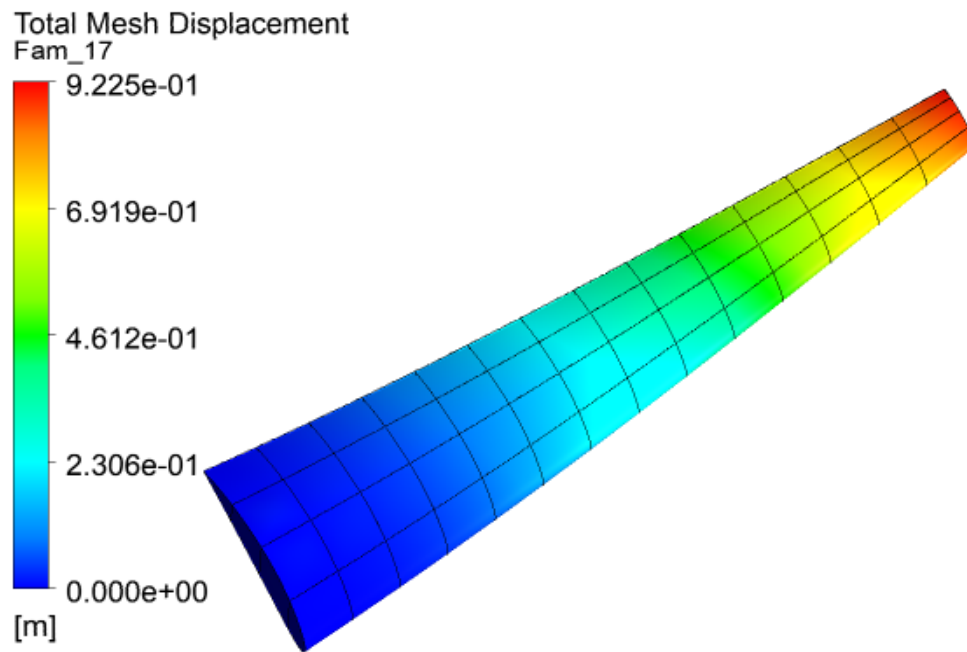


Fig. 3.15. Structural Deformation Using Distributed Load Transfer Method ($\alpha = 7$)

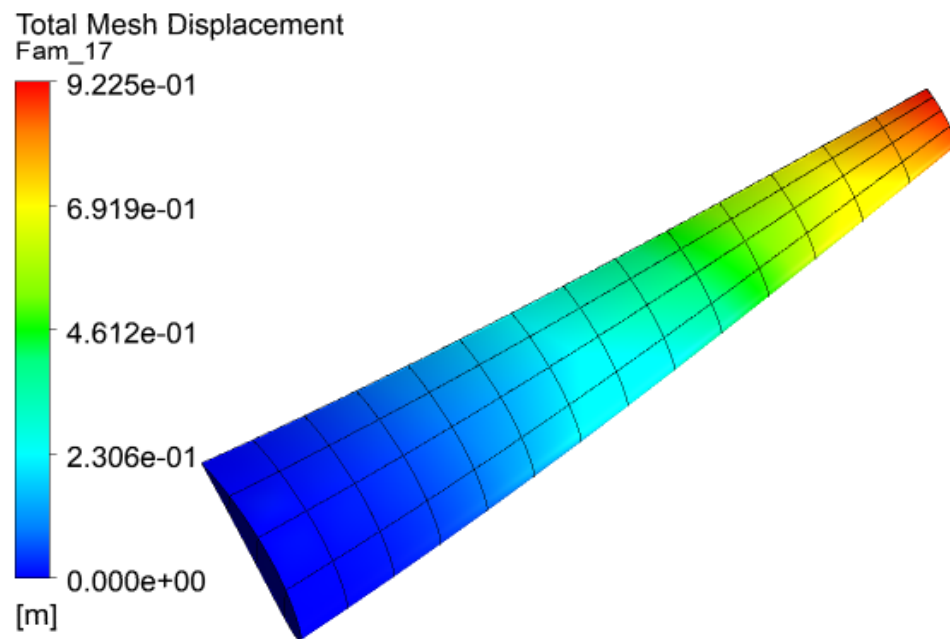


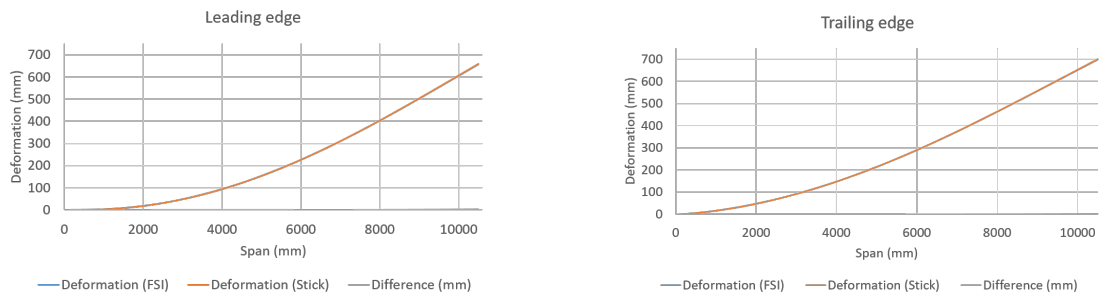
Fig. 3.16. Structural Deformation Using Discretized Load Transfer Method ($\alpha = 7$)



Fig. 3.17. Deformation vs Span at Leading Edge (Alfa = 7)



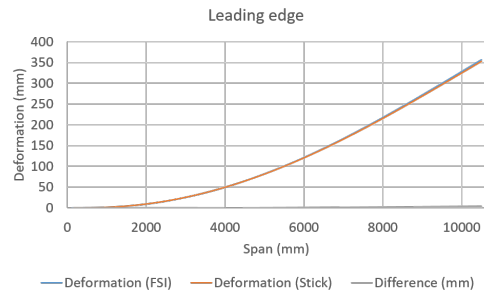
Fig. 3.18. Deformation vs Span at Trailing Edge (Alfa = 7)



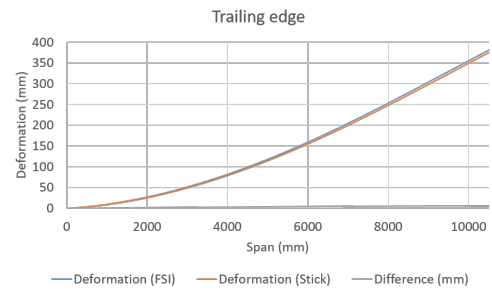
(a) Deformation vs Span at leading edge

(b) Deformation vs Span at trailing edge

Fig. 3.19. Deformation vs Span (Alfa = 4)



(a) Deformation vs Span at leading edge



(b) Deformation vs Span at trailing edge

Fig. 3.20. Deformation vs Span ($\text{Alfa} = 0$)

4. WEIGHT OPTIMIZATION OF WING USING INDIRECT LOAD TRANSFER METHOD

This chapter focuses on the automatization of multi-fidelity optimization of the structural aspects of the wing. ESP is used to create parametric attributed geometry which maintains consistency between structural models with different fidelity levels. A stiffness based strategy is used to map the nodal data of the lower-order fidelity structural models onto the higher-order ones to perform buckling analysis. To demonstrate the approach, a wing is being optimized to withstand with two separate loadcases. An API is created to connect the ESP, Nastran, load file and design configuration file in CSV format.

4.1 User Inputs

To optimize the internal structure, the API takes the geometric and optimization parameters from user in the form of CSV files. The ribs are equally spaced throughout the span. The spars are equally spaced between the first and last spar. In the file user needs to provide the following information:

1. Geometry parameters
 - (a) Area
 - (b) Sweep angle
 - (c) Taper ratio
 - (d) Aspect ratio
 - (e) Fractional distance in the chordwise length for the first spar
 - (f) Fractional distance in the chordwise length for the last spar

2. Load parameters
 - (a) Number of loadcase
 - (b) Factor of Safety (FS) for static structural optimization
 - (c) FS for buckling optimization
3. Number of support member (min and max)
 - (a) Ribs
 - (b) Spars
 - (c) Stiffeners
4. Thicknesses (min and max)
 - (a) Panel
 - (b) Stiffener
 - (c) Rib
 - (d) Spar

In another CSV file, loadcase as shown in Figure 4.1 needs to be provided. Here, +Y is lift direction, +Z is spanwise direction and +X is chordwise direction. The structure can be optimized for any number of loadcases. These loads are total loads on the system at the location. These load cannot be directly applied on the ribs. The conversion of the total load to the applicable load is described in section 3.4 step-6.

4.2 Geometry Script

Here, a detailed method of wing creation and attribution is displayed which is used in further analysis. First, two NACA profiles are created based on parameters provided by the user as it can be seen in Table 4.1. Then they are ruled to create Outer Mold Layer (OML) of wing. The upper surface is attributed as “upper_skin”

	A	B	C	D	E	F	G	H	I
1	Location	0	0.6455	1.291	1.9365	2.582	3.2275	3.873	Stick model node location
2	Fy	85000	72670	60340	48010	35680	23350	11020	
3	Mx	-133550	-111345	-89140	-66935	-44730	-22524	0	Loadcase #1
4	Mz	82420	69250	56080	42910	29750	16580	3410	
5	Fy	-34000	-29068	-24136	-19204	-14272	-9340	-4408	
6	Mx	53420	44538	35656	26774	17892	9009.6	0	Loadcase #2
7	Mz	-32968	-27700	-22432	-17164	-11900	-6632	-1364	
8	Fy								
9	Mx								
10	Mz								
11									
12									

Fig. 4.1. Loadcase CSV File

and lower surface as “lower_skin”. The leading edge and trailing edge are attributed as “leading_edge” and “trailing_edge”. The waffle is created based on parameters of internal structure. The waffle is intersected with solid wing so that the internal structure will have the exact profile of the wing. The waffle is then subtracted from solid wing to create the scribed wing. This scribed wing is then converted to sheet body using “extract” command. The internal structure and sheet wing are unioned to create one continuous structure. While making waffle, each ribs and spars are given attributes. Ribs are identified as name = “Rib” and index = 1,2,3,... as shown in Figure 4.2. The airfoil at the tip is also attributed as Rib with index = nRib+1. The root airfoil is given attribute “Root”. The spars are identified as name = “Spar” and index = 1,2,3,... The panels are identified by the index of rib on the tip side and spar index on the trailing side. For example, as given in Figure 4.3, the panel attribute is U3_2. Here, U is for upper surface; index of the rib on the tip side of panel is 3 and index of the spar on trailing side is 2. All the edges of the panels are also given the attributes of the panel as shown in Figure 4.6. Based on attributes on face of ribs,

spars and panel of the wing, the required edge attributed as “RBE3_1,2,3,...”. The panels attached to trailing edge is given an attribute as “ignoreNode=true” which allows the element associated with the surfaces to not to be present in the Nastran bulk (.bdf) file. This bdf file is used to perform static structural analysis on the wing. Each panel is dumped with extension of .EGADS; later to be imported again into ESP for buckling analysis. The whole flowchart is given in Figure 4.4.

Table 4.1.
Design Parameters of Wing and Panels

Parameter name	Value	Description
series_w	4409	NACA profile of the wing
area	10 m^2	area of the wing
aspect	6	aspect ratio of the wing
taper	0.7	taper ratio of the wing
sweep	20	sweep angle of the wing
nrib	5	number of ribs in the wing
xfirst	0.2	fraction distance in the chordwise length for the first spar
xlast	0.75	fraction distance in the chordwise length for the last spar
nspars	3	number of spars in the wing
nstiff	3	number of stiffeners on the wing panel
depth	-0.01	depth of the stiffener
angle	45	angle of the runoffs at the ends of the stiffener

Further, to optimize the wing for buckling mode, each panel needs to be stiffened. As the stiffeners are discontinuous, they don't play an important role in material failure but they are very important for buckling stability. For that, the dumped panels are imported and are stiffened using a User Defined Function (UDF) called

“stiffeners”. UDF stiffeners create surfaces perpendicular to the local surface on the panel for a given depth. It also generates runoffs at the end of stiffeners. These parameters are also given in Table 4.1

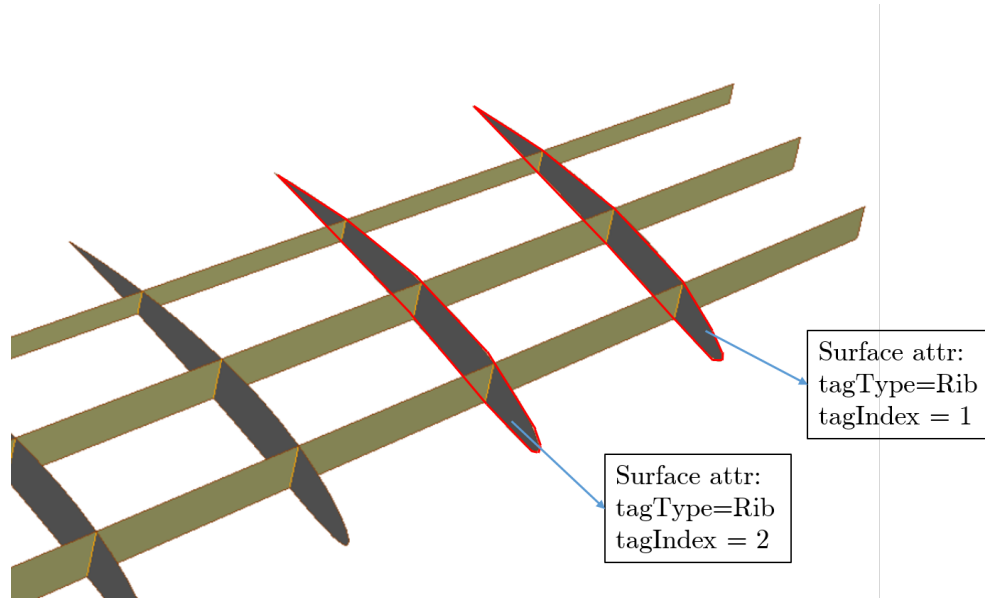


Fig. 4.2. Rib Attributions

4.3 Analysis Setup

To perform optimization automatically, the API works as pre-processor to apply material property, boundary conditions, data transfer between different fidelity, etc. It reads the load data, geometric and optimization parameters from separate CSV files. The API also works as postprocessor and makes the decision about change in the number of structural members. It generates CSM for ESP and gets the attributed mesh from ESP.

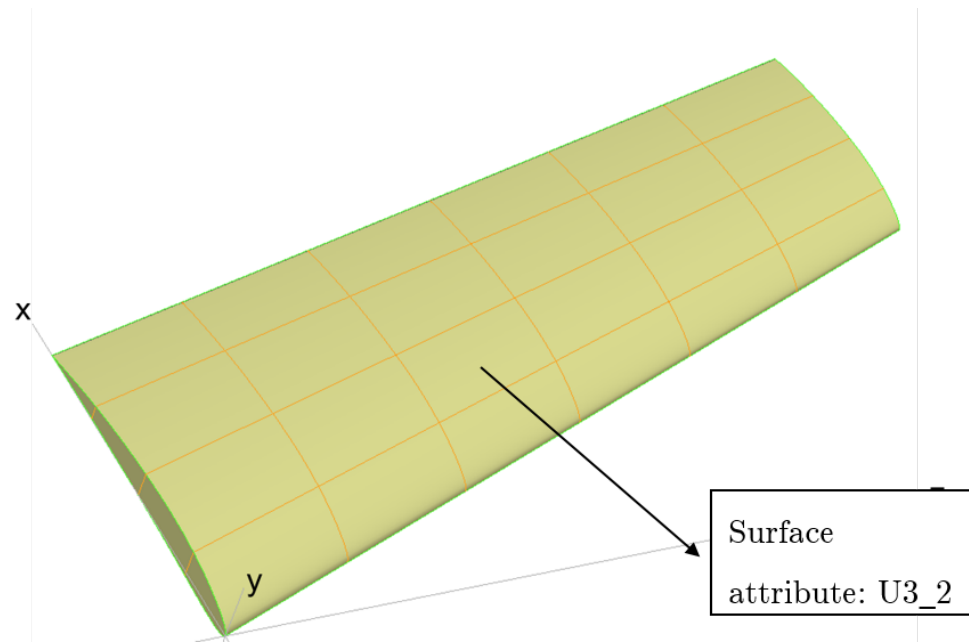


Fig. 4.3. Example of Panel Attribution

4.3.1 Static Structural Failure Mode

After completing the geometry generation and attribution on surfaces, ESP dumps the mesh file in a .bdf format which has attribution on nodes and elements. For the material failure of the wing, in Global Finite Element Model (GFEM), stiffeners are not modeled. As the stiffeners are not continuous, they do not provide rigidity against static failure. In this mesh file, nodes and the elements grouped according to their geometric attributes. Using these attributes, the elements of each panel is identified and given separate property ID (PID). All the ribs are given the same PID and all spars have the same PID. To transfer the load on the wing, RBE3 master nodes are generated at the geometric center of each rib. The edge nodes shown in Figure 4.5 are connected to the master node. These nodes are also identified based on attribution (i.e. RBE3_1, RBE3.2...). Here, a conservative approach is taken in which all the loads are assumed to be taken by wingbox.

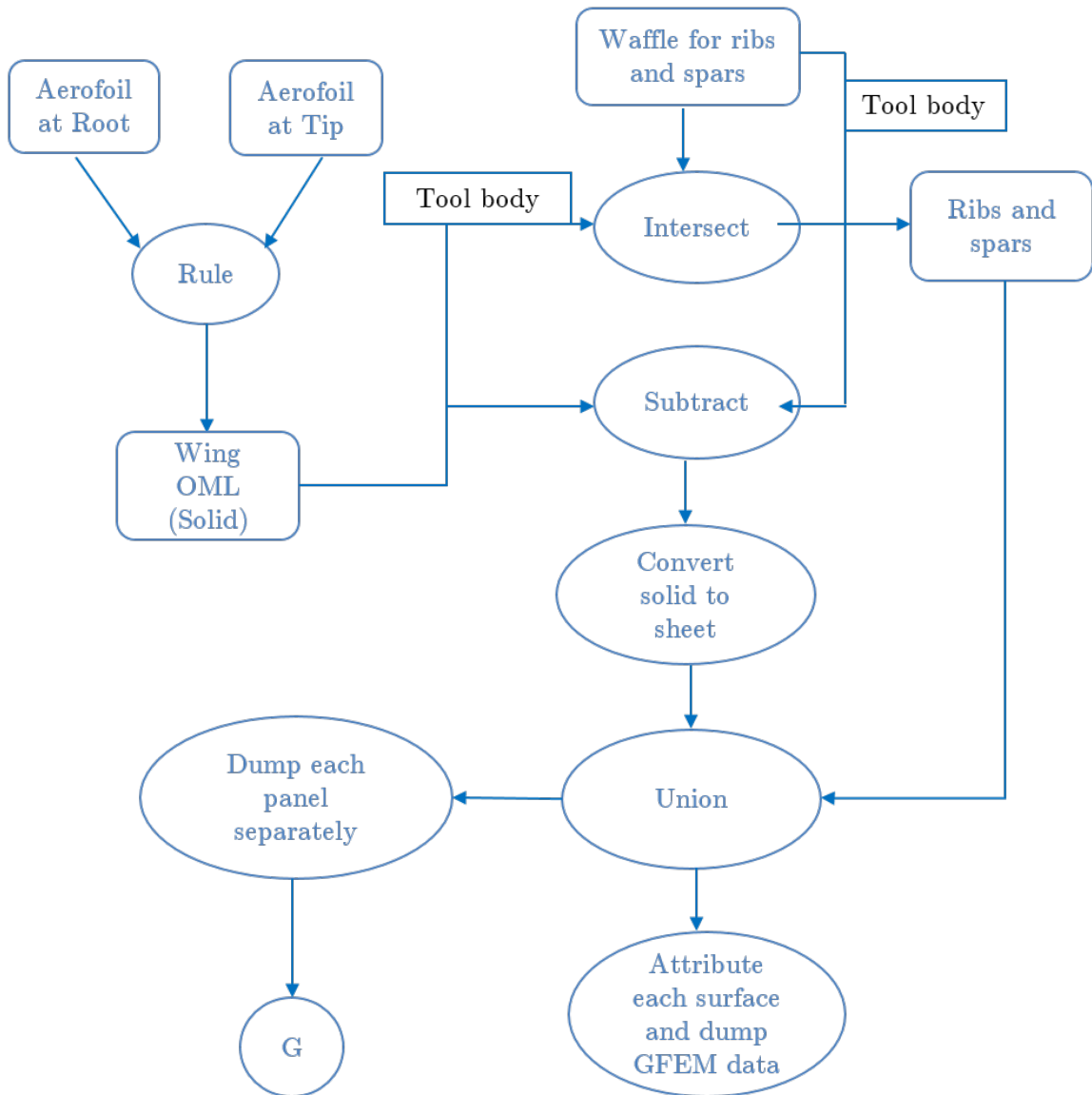


Fig. 4.4. Flowchart for Geometry Script

After differentiating between element properties and generation of new elements, loads can be applied on RBE3 master nodes. The master node distributes the load on slave nodes based on screw theory. These loads are provided by the user in CSV file as shown in Figure 4.1. If the location of stick model nodes and location of

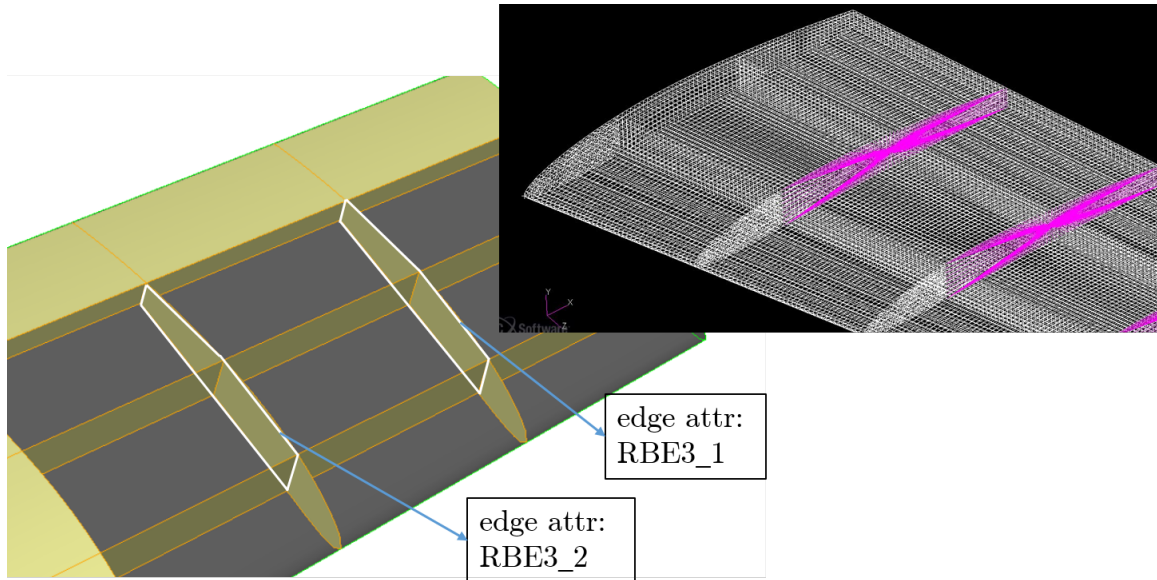


Fig. 4.5. RBE3 Connection

RBE3 master nodes doesn't match, interpolation is done. The root is given fixed constraints. The new bdf file is generated which includes Nastran executive controls, case-control, bulk data, and optimization control data. The optimization control data contains variables (i.e. the thickness of each PID), constraints (i.e. max stress) and an objective function (i.e. minimize weight). The bdf file is sent to Nastran to optimize using SOL 200 for static structural failure mode. The optimization is done on all provided loadcases. The minimum thickness for each PID for n^{th} loadcase is equal to optimized thickness for $(n-1)^{th}$ loadcase. Minimum thickness for 1^{st} loadcase is provided by the user.

4.3.2 Buckling Failure Mode

Further, for buckling stability, the deformation data of each loadcase needs to be transferred from lower fidelity to higher fidelity model for overall optimization. To do that, static structural analysis needs to be performed to get deformation on

GFEM. For the first loadcase of buckling optimization, the thicknesses are equal to the optimized thickness of the last loadcase of static structural optimization. From 2nd loadcase, the thicknesses for nth loadcase are equal to optimized thicknesses of buckling optimization for (n-1)th loadcase. The buckling optimization process is a serial process which means that at one time only one panel is being optimized. For the example shown in Figure 4.6, the panel U3_2 is being optimized. The ID and location of edge nodes which are attributed as U3_2 are stored in a C program structure from GFEM file. Their deformations are also stored from the result file (.f06) of Nastran. The panel is imported and the required number of stiffeners are attached using UDF “stiffeners”. This time, the edge of the panel is attributed as “outside” where the deformation data needs to be transferred and the mesh file is dumped. The node ID and location of “outside” nodes are also stored. Their deformation is calculated from nearest “U3_2” edge nodes. The deformations are given in Tx, Ty, Tz and Rx, Ry, Rz directions. The mesh file is edited to provide enforced displacement on each “outside” nodes and buckling optimization parameters. Here, the panel and stiffeners are given separate PID. All the stiffeners of particular panel share the same PID.

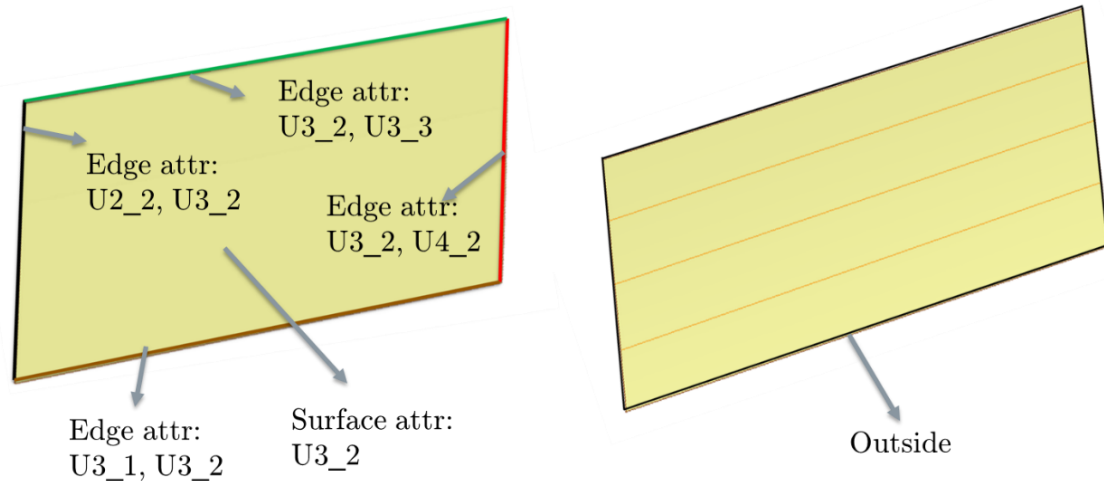


Fig. 4.6. Edge Attributions of Unstiffened and Stiffened Panel

The buckling optimization for each panel is repeated until the maximum number of stiffeners are attached. From this, the combination of thicknesses and number of stiffener which gives minimum weight is selected as the optimized combination for a particular panel. For buckling optimization, the value of the minimum thickness for skin and stiffeners and the minimum number of stiffeners for n^{th} loadcase is equal to optimized parameters for $(n-1)^{th}$ loadcase. The minimum thicknesses of panels for 1^{st} loadcase is equal to optimized thickness for the last loadcase of static structural analysis. Minimum thickness and number of stiffener is defined by user. The process is repeated for all the panels except for ailerons as it is assumed that they don't take any load. The process of buckling optimization is repeated for all the loadcases. The whole process from static structural optimization is repeated for all possible combination of ribs and spars. The combination of thicknesses and number of structural members which satisfy both failure modes and generates minimum weight is selected as optimized design. The flowchart for the analysis process is shown in Figure 4.7.

4.4 Results

The wing with given geometry parameters in Table 4.1 and for loadcases shown in Figure 4.1 is optimized. The constrain is 500MPa with FS for static structural and buckling is 1.2 and 1.1 respectively. The range of thicknesses for all surfaces is 8mm to 1mm. Number of ribs varies from 3 to 6 and number of spars are fixed 3. Number of stiffeners varies from 0 to 4. The results of overall optimized geometry have 5 ribs and 3 spars. The rib thickness is 1.19mm and spar thickness is 4.47mm. the overall weight of the wing is 84.6 KG. The details about the panels are shown in Table 4.2. The results are shown in Figure 4.8 and Figure 4.9.

Table 4.2.: Results of Optimized Geometry

Panel name	Number of stiffeners	Thickness of panel (mm)	Thickness of stiffeners (mm)	Weight (KG)
U1.1	3	2.02	1.07	1.45
U2.1	3	2.53	1.63	1.74
U3.1	3	2.79	1.73	1.78
U4.1	3	2.47	1.64	1.49
U5.1	3	2.10	1.52	1.18
U6.1	3	1.42	1.00	0.72
U1.2	2	4.98	1.00	3.64
U2.2	3	4.33	2.59	3.38
U3.2	3	4.46	2.62	3.32
U4.2	3	4.00	2.51	2.86
U5.2	3	3.71	2.47	2.56
U6.2	3	2.80	1.68	1.80
U1.3	3	3.86	1.56	3.02
U2.3	3	3.13	2.72	2.61
U3.3	3	3.42	3.88	2.89
U4.3	3	3.67	2.92	2.75
U5.3	3	3.28	2.16	2.26
U6.3	3	1.98	1.00	1.23
L1.1	3	2.13	1.00	1.41
L2.1	2	1.97	1.08	1.18
L3.1	3	1.78	1.43	1.13
L4.1	2	1.95	1.42	1.03
L5.1	2	1.69	1.22	0.82
L6.1	0	1.00	1.00	0.34

continued on next page

Table 4.2.: *continued*

Panel name	Number of stiffeners	Thickness of panel (mm)	Thickness of stiffeners (mm)	Weight (KG)
L1.2	2	4.67	1.65	3.50
L2.2	3	3.24	1.00	2.36
L3.2	2	2.87	1.26	1.98
L4.2	3	2.50	1.00	1.69
L5.2	3	1.95	1.00	1.29
L6.2	3	1.55	1.00	1.01
L1.3	2	4.82	1.00	3.52
L2.3	3	2.60	1.39	1.99
L3.3	3	2.14	1.11	1.56
L4.3	3	2.21	1.00	1.51
L5.3	3	1.78	1.00	1.19
L6.3	0	1.00	1.00	0.53

4.5 Conclusion

It is possible to optimize the wing for both the failure criteria without any human input by careful use of attributes. This approach can be applied to the whole aircraft if needed. However, the author suggests to make two layers of API. One API for general purpose analysis in which the user can apply any load on any attributes which can be given using GUI. Another program can be built on top of first API to run the analysis or optimization in a loop.

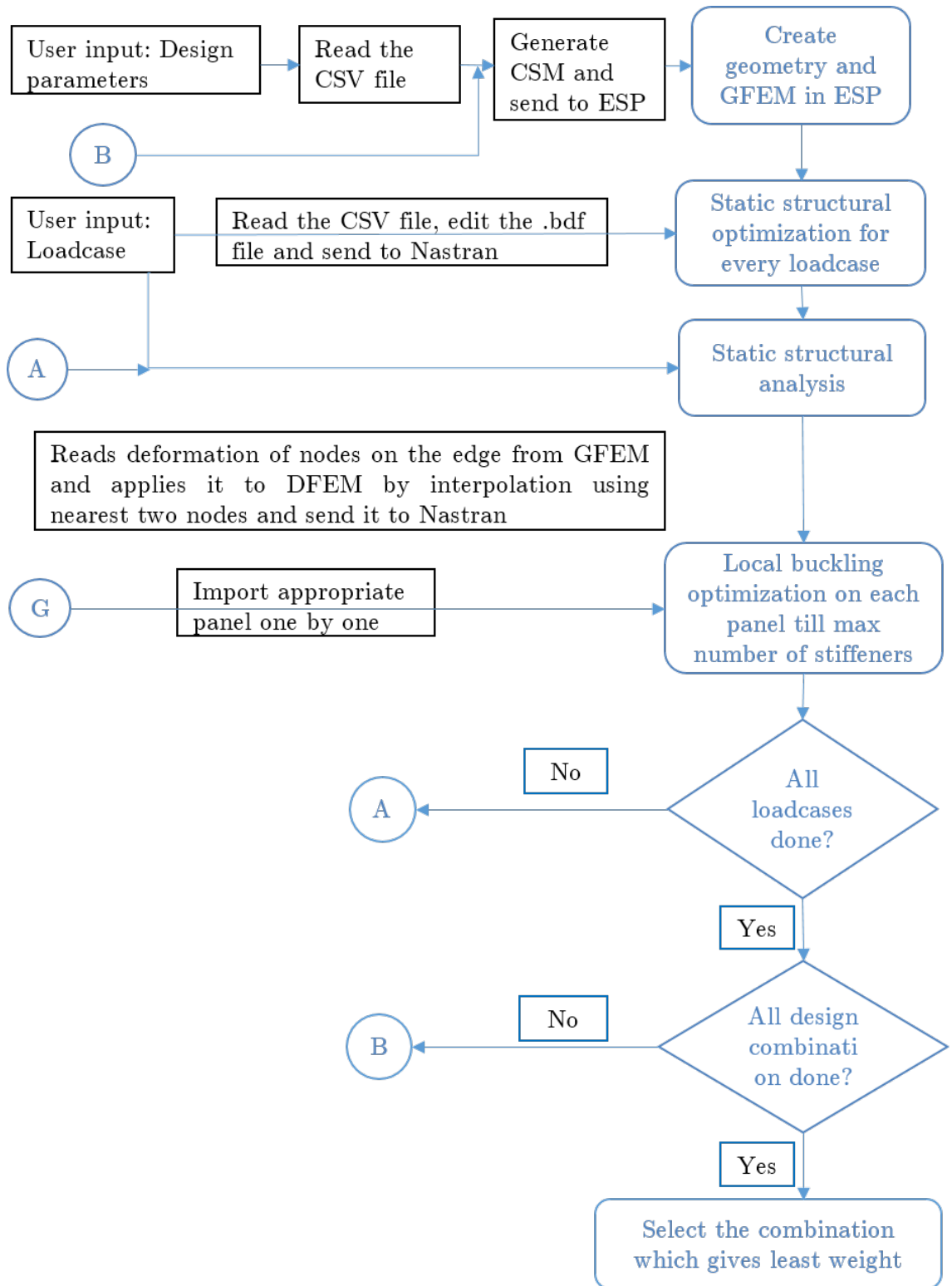


Fig. 4.7. Flowchart for Analysis Process

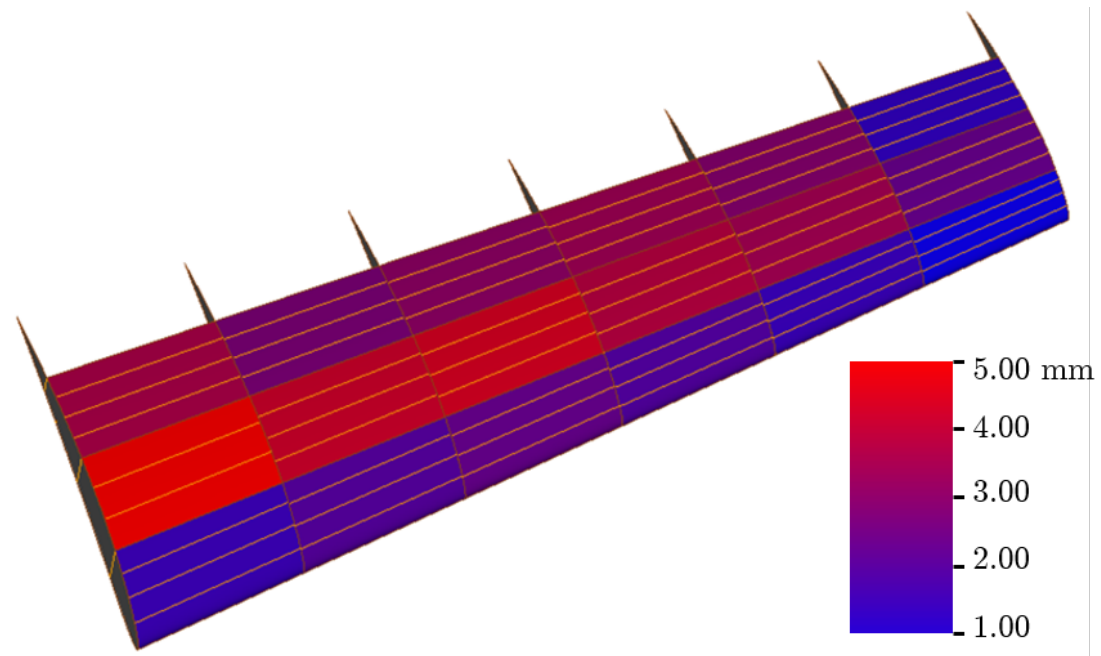


Fig. 4.8. Optimized Upper Surface

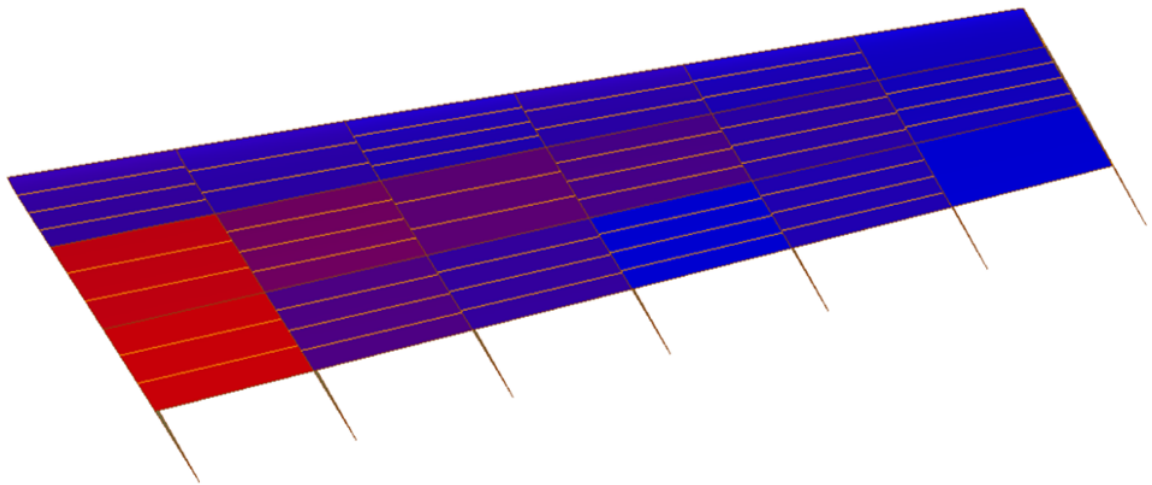


Fig. 4.9. Optimized Lower Surface

5. PARAMETRIC DESIGN OF AIRCRAFT USING ENGINEERING SKETCHPAD (ESP)

In this chapter, a comprehensive method to create a parametric model of aircraft is shown. For commercial aircraft and for fighter aircraft, some techniques are different but the general idea of Outer Mold Layer (OML) and internal structure remains the same. The final goal is to extend the idea of single button optimization of the wing to single button optimization of aircraft and this is the first step in the direction.

5.1 Military Aircraft Prototype Syntheses

The master models in ESP are defined in terms of a feature tree and a set of design parameters. This tree depicts the sequence of the operations used to create the final design which can be extracted from the CSM file and is shown in Figure 5.1.

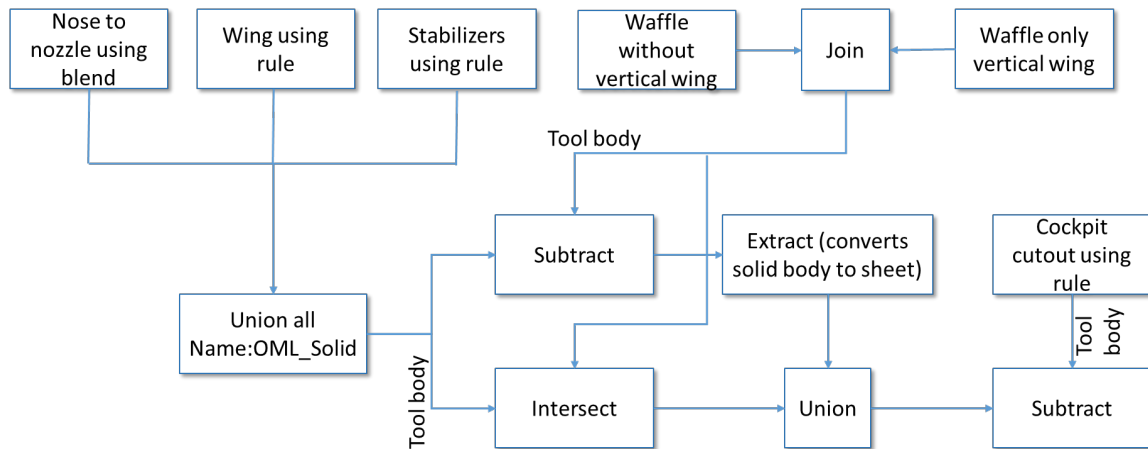


Fig. 5.1. ESP Tree Structure to Generate a Military Fighter Aircraft

In this tree structure, each part contains several steps. These steps are called ‘Branches’. Each part starts with the generation of standard primitives which includes Box, sphere, cone, cylinder, or torus. Some branches are used to grow sketches such as extrude, rule, blend, revolve, sweep, or loft. And some are User Defined Primitives (UDP) such as ‘Naca’ and ‘supell’ (superellipse). ESP arranges bodies in a stack order approach. This means that a given command is being operated on the last generated body or the last two bodies in case of the Boolean operations.

The section “nose to nozzle using blend” is divided into three sections. First, the super-elliptical sheets are created to generate cone section of the body. It all sheets were blended with a nose radius. Second, the cylindrical section is created which is between nose and nozzle. Third, the nozzle section is created and unioned them together shown in Figure 5.2. The wing and the stabilizers are created by creating naca profile at the required location and ruling them together. Then all the parts are unioned to form complete OML represented in Figure 5.3.

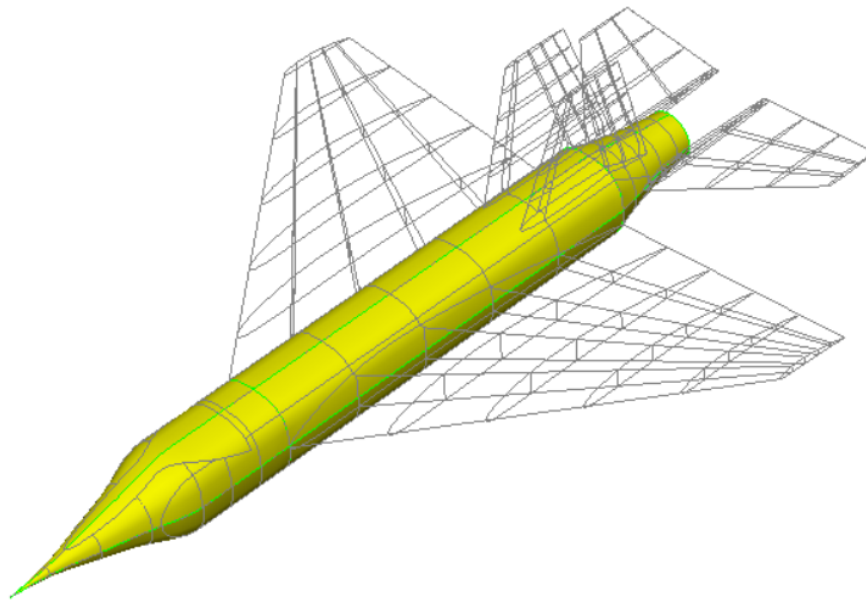


Fig. 5.2. Middle Section of Aircraft

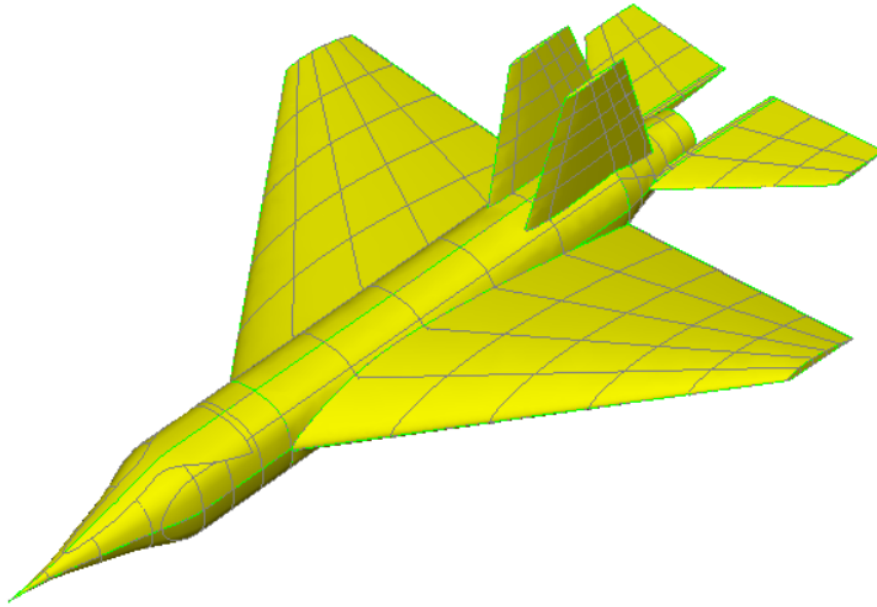


Fig. 5.3. Solid OML

For unibody design of the internal structures, two separate waffles need to be created. One for vertical stabilizers (Figure 5.4) and another for remaining of the structure (Figure 5.5). Both waffle shares line contact with each other and they are connected using the “join” command to generate structure shown in Figure 5.6. This is the key step in the generation of continuous internal structure. The waffle is then subtracted from the OML, which enforces the outer sheet Body to be scribed by the faces of the waffle. The waffle is then intersected with solid OML (non-scribed) to create internal structure with the exact shape of OML (Figure 5.7). The scribed OML is converted to sheet OML and unioned with internal structure. From this unibody, the cockpit section and the engine section are subtracted.

Table 5.1 shows the design parameters used in building the parametric model of the aircraft. The three models shown in Figure 5.8 are different in terms of the configuration of their aerodynamic parameters and internal structures. The design parameters of each model have been depicted in Table 5.2.

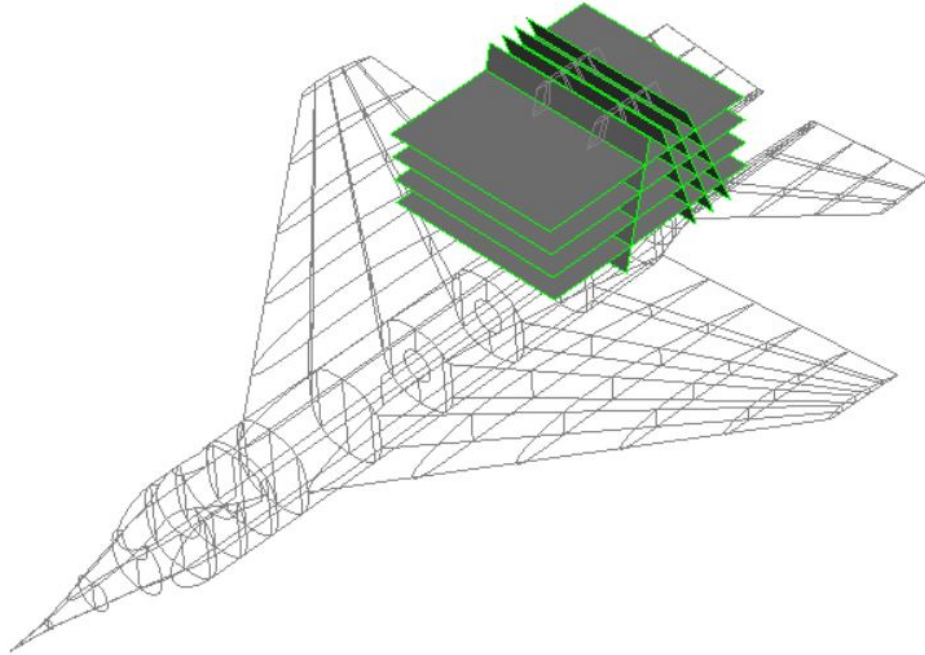


Fig. 5.4. Waffle for Vertical Stabilizer

Table 5.1.: Design Parameters

Parameter name	Value	Description
cone_radius	0.25	Radius of nose cone
cone_length	1.2	Length of nose cone
cockpit_length	5.5	Length of cockpit
cockpit_num	3	Frame number in cockpit
cockpit_width	2.0	Width of cockpit
engine_length	4.5	Length of engine
engine_num	2	Width of engine
engine_width	4.0	Frame number in engine
spars_num	6	Number of spars
spars_initial_length	20.0	Length of wing at root

continued on next page

Table 5.1.: *continued*

Parameter name	Value	Description
spars_final_length	4.0	Length of wing at tip
wing_tip	22.5	Wing tip leading edge distance from nose
wing_span	30.0	Span of wing
nozzle_width	2.8	Initial width of nozzle
nozzle_length	3.0	Length of nozzle
nozzle_out_radius	1.15	Radius of nozzle at exit
nozzle_num	3	Number of frames in nozzle section
series_w	4409	NACA profile
AOA1	2.0	Angle of attack at root
AOA2	5.0	Angle of attack at tip
series_h	406	NACA profile
hwing_start_length	8.0	Length of horizontal wing at root
hwing_end_length	3.0	Length of horizontal wing at tip
hwing_spars_num	3	Number of spars in horizontal wing
hwing_tip	36.0	Horizontal wing tip leading edge distance from nose
hwing_span	15.0	Span of horizontal wing
vwing_height	6.0	Vertical wing tip height from nose
vwing_end_length	3.5	Length of vertical wing at tip
vwing_tip_dist	33.0	Vertical wing tip leading edge distance from nose
mid_ribs	7	Number of ribs in fuselage
wing_ribs	5	Number of ribs in wing
Hwing_ribs	2	Number of ribs in horizontal wing
vwing_ribs	4	Number of ribs in vertical wing

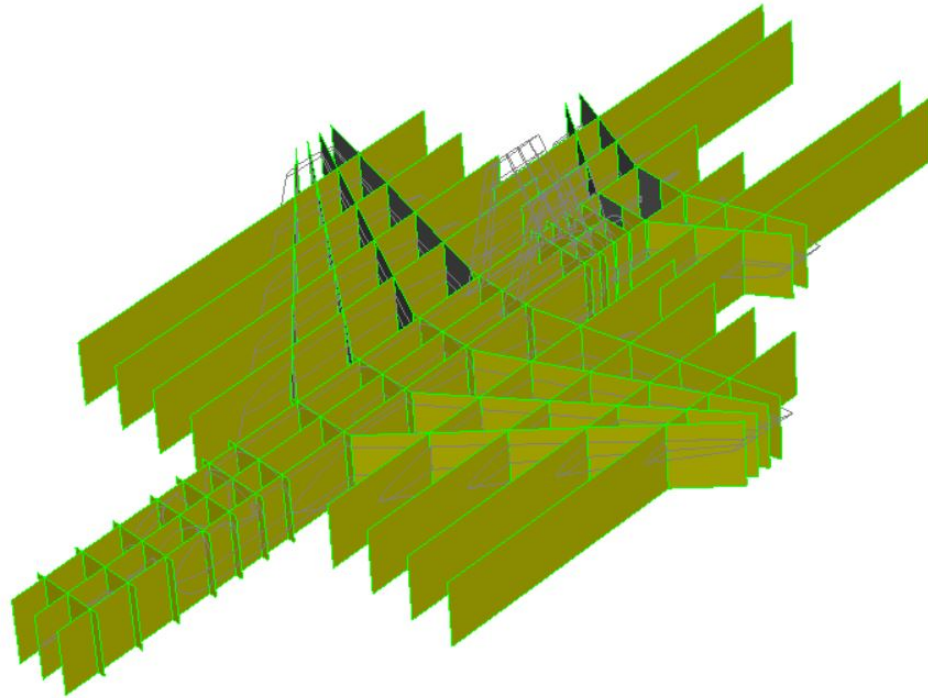


Fig. 5.5. Waffle Without Vertical Stabilizer

Table 5.2.
Design Parameters for Figure 5.8

	Number of Ribs	Number of Spars	Wing tip distance
Figure 5.8.a	3	3	25
Figure 5.8.b	4	4	25
Figure 5.8.c	3	3	22.5

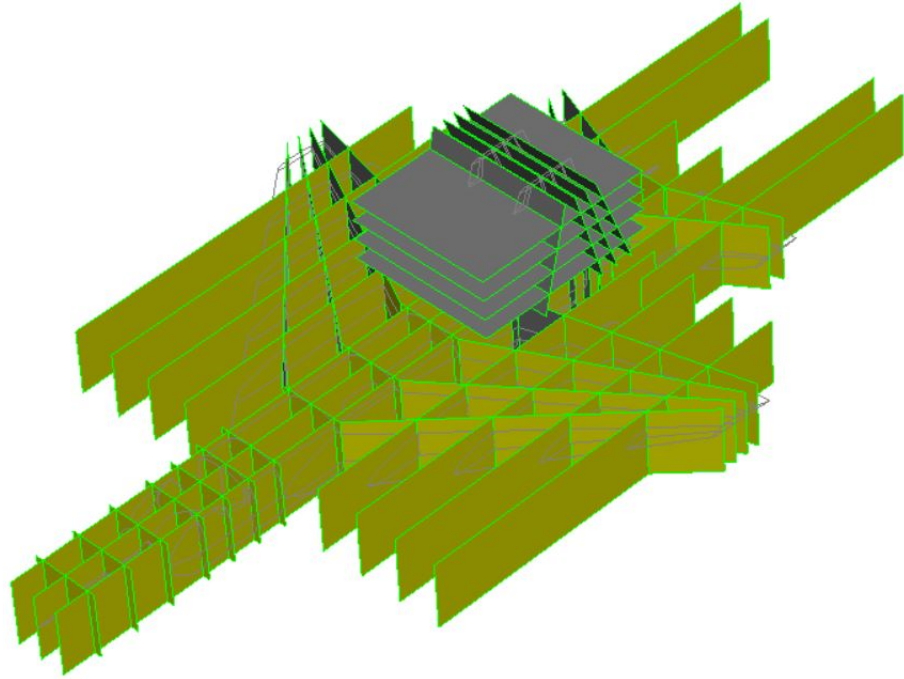


Fig. 5.6. Continuous Waffle

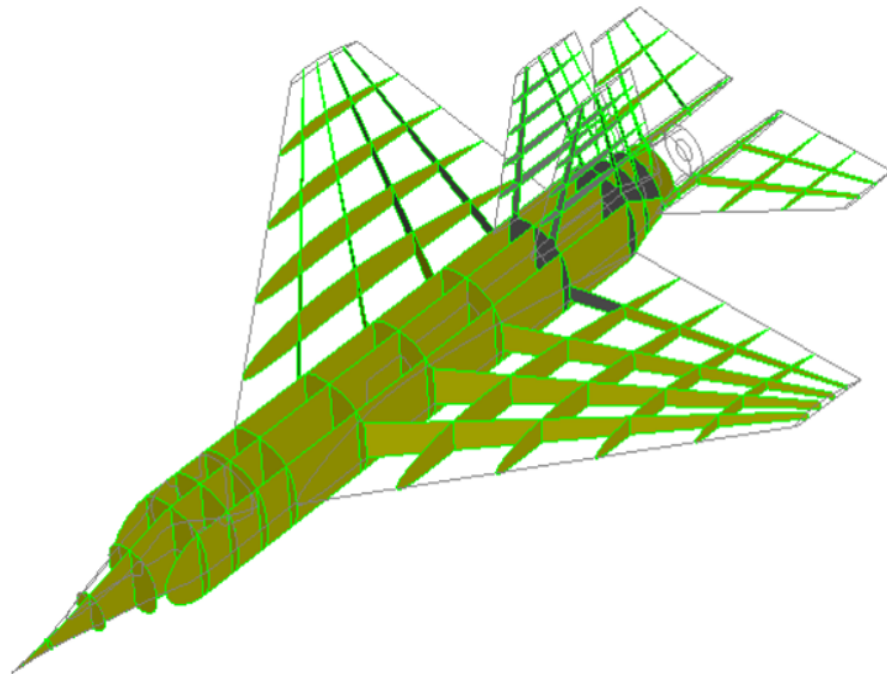


Fig. 5.7. Internal Structure

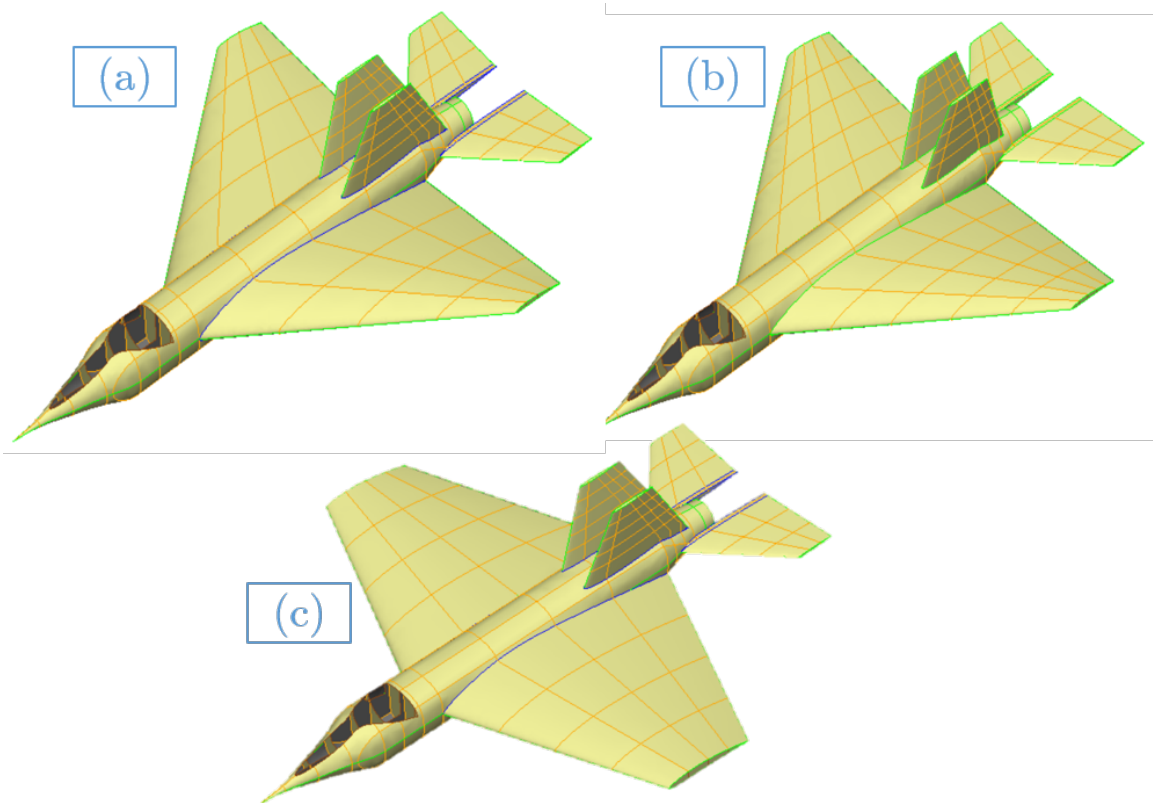


Fig. 5.8. Aircraft with Different Configurations

6. CONCLUSIONS AND FUTURE WORK

6.1 Conclusion

- For low to medium aspect ratio of wing for the preliminary design phase, the discretized load transfer method provides almost the same results as the distributed load transfer method. However, discretization of the load is a relatively tedious process but necessary for the visualization of load characteristics.
- If the design of OML and internal structure; both are being changed iteratively, transferring load using the distributed load transfer method can be preferable.
- Using the attributes of the geometric features as KeyWords, connection between ESP and analysis software is possible by creating appropriate API.
- Automatization of preprocessing and multi-fidelity load transfer can simplify the erring process and can save time.
- Parametric design method is very useful when creating a family of products which shares the same geometric features. However, this approach might be overkill if a quick investigation of 3D design needs to be done at a conceptual phase.

6.2 Future Scope

- Extension of the single button optimization on the whole aircraft
- Methods to transfer load from wing to fuselage needs to be developed and applied to analyze the whole jet simultaneously.
- The optimization of panels can be done in parallel.

- Instead of tailoring API for specific analysis, a general purpose API to connect ESP and Nastran can be created. This API can apply loads, BC and properties based on attributes.
- This API can be created to connect with different solver and not only structural solver but fluid solvers also.
- The general purpose API can be used to couple fluid analysis and structural analysis to perform one-way or two-way FSI for the detailed design phase.

REFERENCES

REFERENCES

- [1] B. Rose, G. Jinu, and M. Manivel, “Partly coupled fluid structure interaction analysis of an aircraft wing at subsonic speeds,” *International Journal of Mechanical & Mechatronics Engineering*, vol. 14, no. 3, pp. 22–29, 2014.
- [2] V. Gandhi, J. Joe, J. Dannenhoffer, and H. Dalir, “Multifidelity structural design and analysis of aircraft structures using engineering sketch pad and nastran,” in *AIAA Scitech 2020 Forum*, January 2020.
- [3] R. Haimes and J. Dannenhoffer, “The engineering sketch pad: A solid-modeling, feature-based, web-enabled system for building parametric geometry,” in *21st AIAA Computational Fluid Dynamics Conference*, 2013, p. 3073.
- [4] Nasa Glenn Research Center, *Boundary Layer*, (accessed July 20, 2019). [Online]. Available: <https://www.grc.nasa.gov/WWW/k-12/airplane/boundlay.html>
- [5] F. M. White, *Viscous fluid flow*, 3rd ed. McGraw-Hill New York, 2006, pp. 75–78.
- [6] Pointwise, *Y+ Calculator*, (accessed July 20, 2019). [Online]. Available: <http://www.pointwise.com/yplus/>
- [7] Autodesk, *SST K- ω Turbulence Model*, (accessed July 20, 2019). [Online]. Available: <https://knowledge.autodesk.com/support/cfd/learn-explore/caas/CloudHelp/cloudhelp/2014/ENU/SimCFD/files/GUID-0F5C4828-9F91-46B6-A16A-2578D72DCFCC-htm.html>
- [8] Ansys, *FLUENT 6.3 User’s Guide - 12.5.2 Shear-Stress Transport (SST) - Model*, (accessed July 20, 2019). [Online]. Available: <https://www.sharcnet.ca/Software/Fluent6/html/ug/node487.htm>
- [9] H.-J. Bungartz and M. Schfer, *Fluid-Structure Interaction: Modelling, Simulation, Optimisation*. Springer, 01 2006.
- [10] Ansys, *Ansys Coupling User Guide*. Ansys User Guide, 2016, pp. 65–72.
- [11] P. Galpin, R. Broberg, and B. Hutchinson, “Three-dimensional navier stokes predictions of steady state rotor/stator interaction with pitch change,” in *Proceedings of 3rd Annual Conference of the CFD Society of Canada, Banff, AB, Canada*, vol. 3, 1995.
- [12] Mike and A. Canard, *XFLR5*, (accessed July 20, 2019). [Online]. Available: http://www.apollocanard.com/6_xflr5.htm
- [13] S. Batchu, *RBE2 Vs RBE3*, (accessed July 20, 2019). [Online]. Available: <http://www.stressebook.com/rbe2-vs-rbe3/>

- [14] Quartus Engineering, *NASTRAN 101*, (accessed July 20, 2019). [Online]. Available: <https://www.quartus.com/resources/nastran-101>
- [15] MSC.software, *Nastran Quick Reference Guide*. MSC.software, 2017.
- [16] MSC.software, *Design Optimization*, (accessed July 20, 2019). [Online]. Available: <https://www.mscsoftware.com/application/design-optimization>
- [17] M. Brunelli, *Parametric vs. Direct Modeling*, (accessed July 20, 2019). [Online]. Available: <https://www.ptc.com/en/cad-software-blog/parametric-vs-direct-modeling-which-side-are-you-on>
- [18] DesignTech, *Parametric Modelling, Process, Advantages and Parametric Modelling Tools*, (accessed July 20, 2019). [Online]. Available: <https://www.designtechsys.com/articles/parametric-modelling>
- [19] J. Dannenhoffer, “Opencsm: An open-source constructive solid modeler for mdao,” *51st AIAA Aerospace Sciences Meeting including the New Horizons Forum and Aerospace Exposition*, no. 0701, 2013.
- [20] R. Haimes and M. Drela, “On the construction of aircraft conceptual geometry for high-fidelity analysis and design,” in *50th AIAA Aerospace sciences meeting including the new horizons forum and aerospace exposition*, 2012, p. 683.
- [21] OPEN CASCADE, *OpenCascade*, (accessed July 20, 2019). [Online]. Available: <http://www.opencascade.org>
- [22] Wikiwand, *Wikiwand*, (accessed July 20, 2019). [Online]. Available: [https://www.wikiwand.com/en/Chord_\(aeronautics\)](https://www.wikiwand.com/en/Chord_(aeronautics))
- [23] C. L. Ladson, C. W. Brooks, and A. S. Hill, “Computer program to obtain ordinates for naca airfoils,” NASA Technical Memorandum, Report, 1996. [Online]. Available: <https://ntrs.nasa.gov/archive/nasa/casi.ntrs.nasa.gov/19970008124.pdf>
- [24] AirfoilTools, *NACA 4 digit airfoil generator*, (accessed July 20, 2019). [Online]. Available: <http://airfoiltools.com/airfoil/naca4digit>
- [25] S. Hiremath and A. Malipatil, “Cfd simulation of aircraft body with different angle of attack and velocity,” *International Journal of Innovative Research in Science, Engineering and Technology*, vol. 3, 2014.
- [26] D. Creech, *Can someone explain the Y plus value*, (accessed July 20, 2019). [Online]. Available: <https://www.cfd-online.com/Forums/main/861-can-someone-explain-y-plus-value.html>
- [27] SAS IP, *2.3.3.Using Inlets, Outlets and Openings*, (accessed July 20, 2019). [Online]. Available: https://www.sharcnet.ca/Software/Ansys/16.2.3/en-us/help/cfx_mod/i5500692.html
- [28] M. Thurber, *Bombardier Challenger 300 - Wikipedia*, (accessed July 20, 2019). [Online]. Available: https://en.wikipedia.org/wiki/Bombardier_Challenger_300